Three-dimensional printing of continuous plant fiber composites

4

Svetlana Terekhina[1] *and Lamine Hattali*[2]
[1]Arts et Métiers Institute of Technology, LAMPA, Angers, France, [2]Université Paris-Saclay, CNRS, FAST, Orsay, France

4.1 Introduction

Nowadays, researchers around the world are aware of the importance of protecting the atmosphere and biodiversity, by enhancing the sustainability and quality of eco-friendly products. Due to renewable resources and biodegradable behavior, more and more attention has been paid to reinforcing plastics with plant fibers instead of synthetic ones (Li et al., 2020; Karimah et al., 2021; Yan et al., 2014). Interest in natural fiber is associated with economic factors since they are lightweight and thus have low density, high specific strength, and modulus, and their cost is lower in comparison to glass fiber and other synthesized fiber-reinforced composite materials. They also have another important advantage—the possibility of processing and reuse. All of that makes them important materials for the development of a green and sustainable economy. They have been used successfully in construction and engineering, textiles, biomedical applications, biosensors, and smart packaging (Li et al., 2020; Karimah et al., 2021; Yan et al., 2014; Williams, 1990).

The introduction and emergence of three-dimensional (3D)-printing technologies, also referred to as additive manufacturing (AM), into the manufacturing of continuous plant fiber composites opens completely new possibilities for solving the challenges and limitations of conventional processes. For example, the production of highly complex shapes with, interconnected holes or lattice-like geometry, represents a challenge that becomes complicated, if not impossible, or expensive produce using conventional processes. For this reason, manufacturing eco-friendly composite products with complex and delicate shapes that require minimal additional machining and time is extremely important and promising.

AM is defined as a process of adding materials to fabricate objects from CAD models in successive layers (ISO, ASTM; Gibson et al., 2015; Terekhina et al., 2021; Terekhina et al., 2020a). This technology enables the fabrication of complex monolithic structures and geometries, with micrometer resolution, without using expensive tools or molds. It is expected to revolutionize the manufacturing of components. Currently, the most commonly used 3D-printing technique for printing continuous natural fiber-reinforced composites is fused filament fabrication (FFF) or its trademarked alternative fused deposition modeling (FDM) (Additive Manufacturing, 2015; Guo and Leu, 2013; Zhang et al., 2020; Terekhina et al., 2022;

Additive Manufacturing of Polymer-Based Composite Materials. DOI: https://doi.org/10.1016/B978-0-443-15917-6.00004-9

Kuschmitz et al., 2021). The FFF continuous natural fiber printing could be classified into three techniques: (1) filament extrusion, (2) in situ impregnation, and (3) in situ co-extrusion (see Fig. 4.1).

The common natural fibers used in the FFF to print continuous polymer-based composites are: flax (Zhang et al., 2020; Terekhina et al., 2022; Kuschmitz et al., 2021; Le Duigou et al., 2019; Long et al., 2021; Yao et al., 2020), jute (Matsuzaki et al., 2016), pineapple leaf (Suteja et al., 2020), banana (Rivero-Romero et al., 2023), ramie (Cai, Wen, et al., 2022; Cheng et al., 2021), and many others in the case of discontinuous fiber-reinforced composites (Ahmad et al., 2022; Stoof and Pickering, 2018; Depuydt et al., 2019; Lee et al., 2021; Rajendran Royan et al., 2021; Agaliotis et al., 2022). Natural fibers are a cheaper and greener alternative to reinforce the polymer matrix during FFF 3D printing. However, improving the performance of the thermoplastic composites reinforced by plant fibers requires the selection of reasonable processing conditions, taking into account the natural characteristics of both constituents themselves (Balla et al., 2019; Kabir et al., 2020; Ahmed et al., 2020): (1) natural variability (material origin and own growth anisotropy), and (2) the instability of their thermal and moisture absorption properties

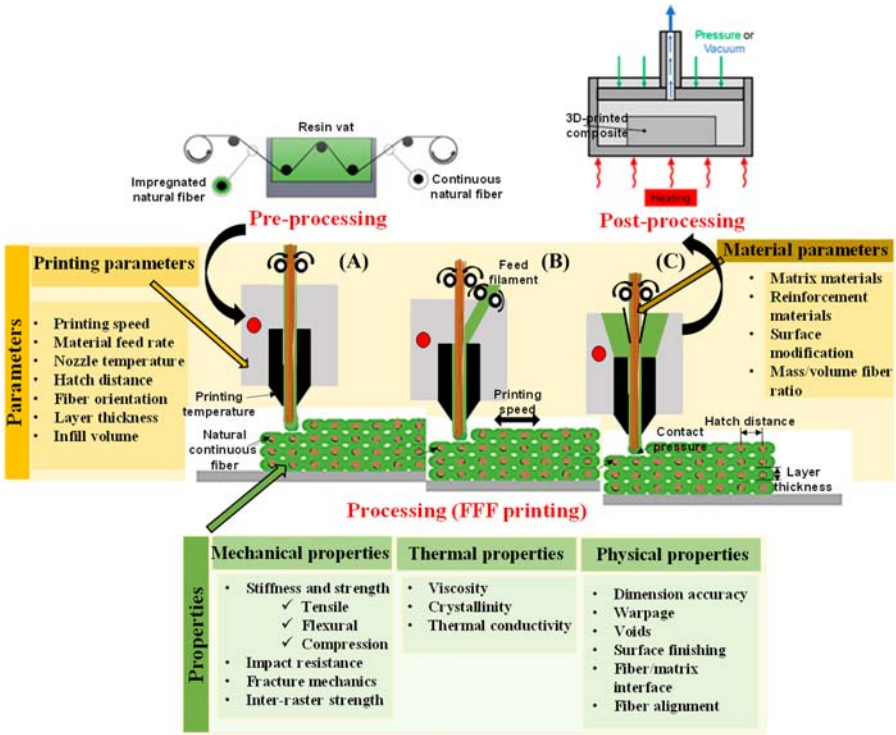

Figure 4.1 Investigated parameters and properties during the FFF process of continuous plant fiber reinforced composites. (A) Filament extrusion, (B) In situ impregnation, and (C) In situ co-extrusion.

(Le Duigou et al., 2020). Unfortunately, defects such as fiber agglomeration (Agaliotis et al., 2022), clogging in the nozzle (Ahmed et al., 2020; Kariz et al., 2018), poor fiber-matrix interface, void content (Terekhina et al., 2022; Matsuzaki et al., 2016; Agaliotis et al., 2022; Balla et al., 2019), and nonhomogeneous mixing (Balla et al., 2019; Kabir et al., 2020; Ahmed et al., 2020) in these composites limit the enhancement of their mechanical performance. Various chemical and thermal treatments are required to be applied to natural fibers to achieve good fiber-matrix and interlayer bonding, fiber homogeneity, and alignment to minimize porosity (Long et al., 2021; Balla et al., 2019; Ravi et al., 2016; Tran et al., 2022; Bhagia et al., 2021).

It is therefore imperative to review the current research trends in 3D printing of continuous plant fiber reinforced composites to understand the cutting-edge tendencies of research in the field, its advantages, and limitations. This chapter aims to summarize and review the current state of research on continuous natural fiber reinforced composites (CNFRCs). It first gives an overview of the technology landscapes existing in the FFF process and subsequently discusses the influence of material and printing parameters, as well as reinforcement geometry and stacking orientation, on the mechanical properties, as well as the challenges of printing complex shapes with continuous fiber orientation. Finally, future trends and applications will be demonstrated (Fig. 4.1).

4.2 Technology landscape

The FFF process is particularly widespread because of its simplicity, relatively high speed, low cost, and the potential for reinventing the designs (ISO/ASTM; Mashayekhi et al., 2021). When manufacturing continuous natural fiber-reinforced polymer composites (CNFRCs), the techniques used to embed the fiber into a thermoplastic matrix influence the mechanical properties of the printed parts. Three techniques are commonly used to print continuous bio-composites in the FFF process: (1) filament extrusion, (2) in situ impregnation, and (3) in situ co-extrusion. (Fig. 4.2 illustrates the schematics of these approaches). The difference is based on the method and timing of introducing the polymer matrix and the fiber into contact with each other. However, the technology landscape described indicates that the FFF process for bio-composites is in its early stages of maturation, with significant potential for growth and development.

- **Filament extrusion**

  Filament extrusion involves two distinct steps to obtain the composite material: (1) impregnation, usually obtained using the extrusion technique of dry continuous fibers with a thermoplastic polymer to form a towpreg, and (2) heating this towpreg during extrusion using a single nozzle head on an open-source 3D printer, before it is deposited on the printing bed (Fig. 4.2A–D). The extrusion impregnation technique commonly employs a single screw extruder and composite extrusion mold, as presented in Fig. 4.2A–C (Zhang et al., 2020). The advantage of this process is that it controls the

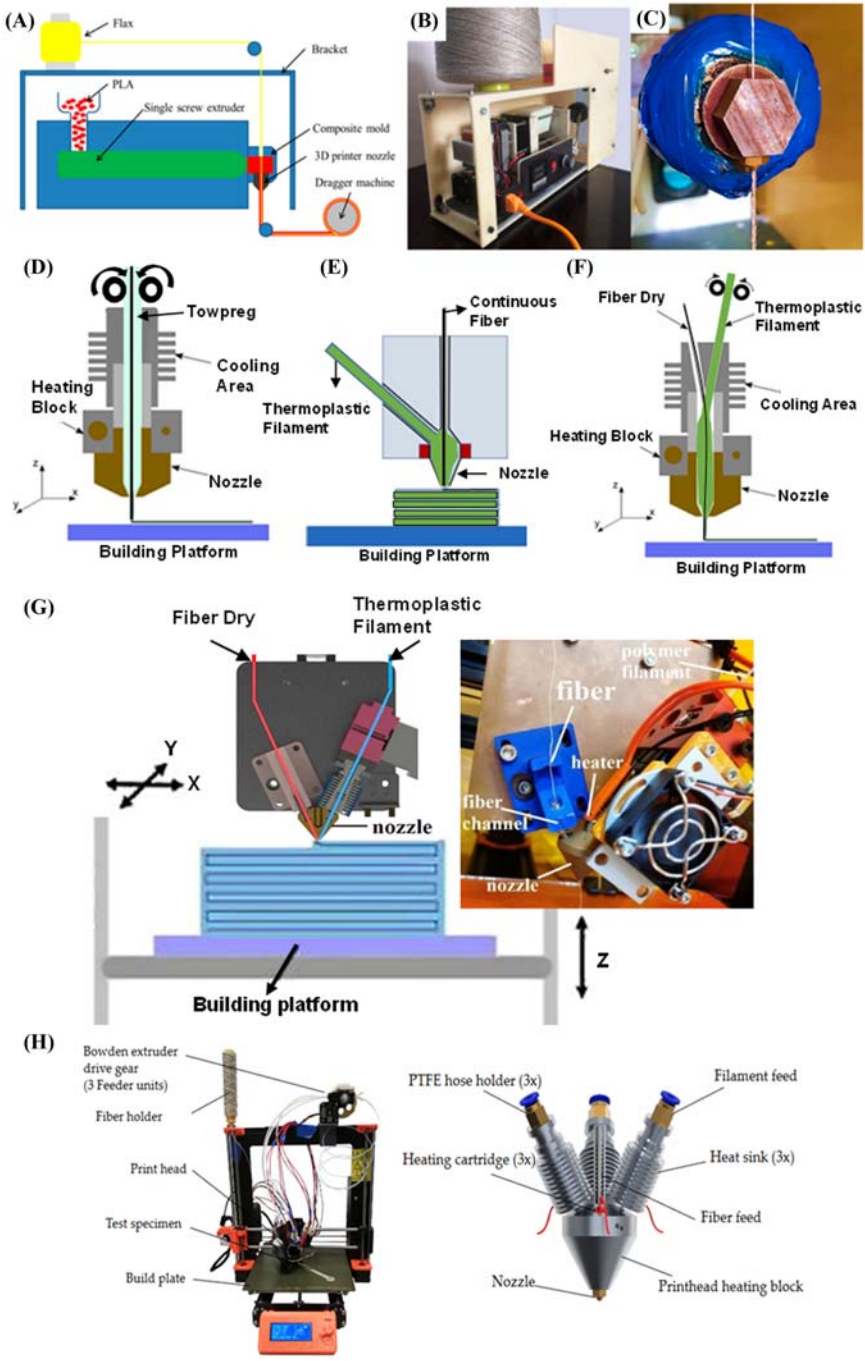

Figure 4.2 Technology landscape in the FFF process of CNFRCs: (A) Schematic and (B) Device (with composite mold); (C) for manufacturing towpreg filament (Zhang et al., 2020); (D-F) Schematic of filament extrusion and in situ impregnation techniques with two ways to

(*Continued*)

filament towpreg over each step, by offering the opportunity to evaluate various polymer matrix/towpreg combinations (Zhang et al., 2020; Le Duigou et al., 2019; Yao et al., 2020; Hu et al., 2018; Vaneker, 2017). The possible disadvantages are plant fiber degradation due to additional thermal stresses that the fiber supports during towpreg production.

- **In situ impregnation**

  In the case of in situ impregnation, the continuous dry filament is fed using two separate channels followed by their mixing in the small heated zone before extruding from a flat-head nozzle (Fig. 4.2E–G) (Terekhina et al., 2022; Long et al., 2021; Matsuzaki et al., 2016; Suteja et al., 2020; Rivero-Romero et al., 2023; Cai, Wen, et al., 2022; Cheng et al., 2021; Zhang et al., 2023). There are different ways of incorporating the dry fiber into the extruder system of the FFF process. The primary objective is to achieve the best fiber/matrix impregnation. This method offers several advantages: (1) ensures thorough mixing of the fiber and the thermoplastic polymer in the heated zone, allowing better fiber distribution and impregnation, (2) controls the composite part volume fraction by varying the flow rates, and (3) allows for one-shot printing of the composite, saving time for industrial applications. However, despite being considered a rapid process, the literature reviews show that parts produced using this method could contain defects (Terekhina et al., 2022; Rivero-Romero et al., 2023).
- **In situ co-extrusion**

  The in situ co-extrusion process consists of feeding the polymer matrix and a towpreg or a continuous yarn separately into the print head (Fig. 4.2H). The melted polymer matrix impregnates the reinforcement, and the obtained composite is deposited by co-extrusion (Kuschmitz et al., 2021). The polymer matrix is generally identical to that of the towpreg.

4.3 Composite material parameters

Many studies were conducted to show the effect of the natural short fiber content on the mechanical properties of the composite obtained by the filament extrusion technique during the FFF process. These plant fibers are derived from oil palm (Ahmad et al., 2022), banana (Singh et al., 2017), henequen (Agaliotis et al., 2022),

◀ incorporate the dry fiber in the extruder system; (G) Example of in situ impregnation technique (Terekhina et al., 2022); (H) Example of in situ co-extrusion process (Kuschmitz et al., 2021). *Source:* From Zhang, H., Liu, D., Huang, T., Hu, Q., & Lammer, H. (2020). Three-dimensional printing of continuous flax fiber-reinforced thermoplastic composites by five-axis machine. *Materials*, *13*, 1678. https://doi.org/10.3390/ma13071678; Terekhina, S., Egorov, S., Tarasova, T., Skornyakov, I., Guillaumat, L., & Hattali, M. L. (2022). In-nozzle impregnation of continuous textile flax fiber/polyamide 6 composite during FFF process. *Composites Part A: Applied Science and Manufacturing*, *153*, 106725. https://doi.org/10.1016/j.compositesa.2021.106725; Kuschmitz, S., Schirp, A., Busse, J., Watschke, H., Schirp, C., & Vietor, T. (2021). Development and processing of continuous flax and carbon fiber-reinforced thermoplastic composites by a modified material extrusion process. *Materials*, *14*, 2332. https://doi.org/10.3390/ma14092332.

kenaf (Saba et al., 2015), or pineapple (Jagadish et al., 2020) trees, as well as from wood (Zhang et al., 2017), bamboo (Depuydt et al., 2019; Wang et al., 2014), ramie (Yu et al., 2015), hemp, or harakeke fibers (Stoof and Pickering, 2018). They could be obtained as harvested or industrial waste products. They increase the mechanical properties of the neat polymers. In addition, many investigations have been conducted in the processing of continuous synthetic fibers using different techniques of their impregnation by the FFF process, underscoring significant interest in its development (Hu et al., 2018; Vaneker, 2017; Pruß and Vietor, 2015). However, the 3D printing of CNFRCs has not received as much attention so far due to the various difficulties to obtain them, but it is still a work in progress. Continuous flax-reinforced polylactic acid (PLA) composites are commonly used for printing continuous bio-composites (Zhang et al., 2020; Kuschmitz et al., 2021; Le Duigou et al., 2019; Long et al., 2021; Yao et al., 2020; Le Duigou et al., 2020). Additionally other materials such as bananas (Rivero-Romero et al., 2023), pineapple leaf (Suteja et al., 2020), jute (Matsuzaki et al., 2016), or ramie (Cai, Wen, et al., 2022; Cheng et al., 2021) are also utilized for reinforcing bio-composites through 3D printing. It is also worth mentioning rare instances such as bleached flax/PA6 composites (Terekhina et al., 2022).

Figs. 4.3 and 4.4 show graphical overviews of the tensile properties versus volume or mass fraction fiber for unidirectional (UD) composites reinforced with different plant fibers obtained by the FFF process. The elastic modulus and tensile strength vary in the range of 0.6−15.6 GPa and 44−186 MPa, respectively. However, it is important to note the remarkable strengths achieved with PLA reinforced by flax (186 MPa) and pineapple leaf (93 MPa) fibers, attributed to both high-quality fiber content and the composite FFF technique. The best result in elastic modulus was obtained for the UD flax/PLA composite.

More details of the mechanical properties, including tensile and flexural strength and stiffnesses, as well as the properties of flax/PLA, flax/polypropylene (PP), flax/PA11, flax/epoxy, flax/polyester, or hemp/PLA composites obtained by conventional processes, are provided in Table 4.1. There is a large amount of literature detailing the mechanical performance of natural fiber reinforced composites obtained by conventional processes (Pickering et al., 2015; Shah, 2013; Gautreau et al., 2021; Marrot et al., 2014; Oksman, 2001; Coroller et al., 2013; Baghaei et al., 2014; Bourmaud et al., 2016; Monti, 2016; Pantaloni et al., 2021; Couture et al., 2016). UD flax/PLA composites obtained by the FFF process provide, on average, an equivalent fiber linear density (~100 tex) and about the same tensile strength as UD flax/PLA composites obtained by the thermocompression process, but their Young's modulus is ~40% as low (15.9 GPa according to Gautreau et al., 2021). Concerning the highest tensile values obtained for the FFF-printed UD flax/PLA composites, the results of elastic modulus are in accordance with Gautreau et al. (2021), and their tensile strength is even ~40% as high (186 MPa). The same trend was observed in comparison with UD flax/epoxy and UD flax/polyester composites obtained by conventional processes (Marrot et al., 2014; Oksman, 2001; Coroller et al., 2013). For the equivalent fiber volume content, their range of tensile properties (130−224 MPa and 11−18 GPa for tensile strength and modulus,

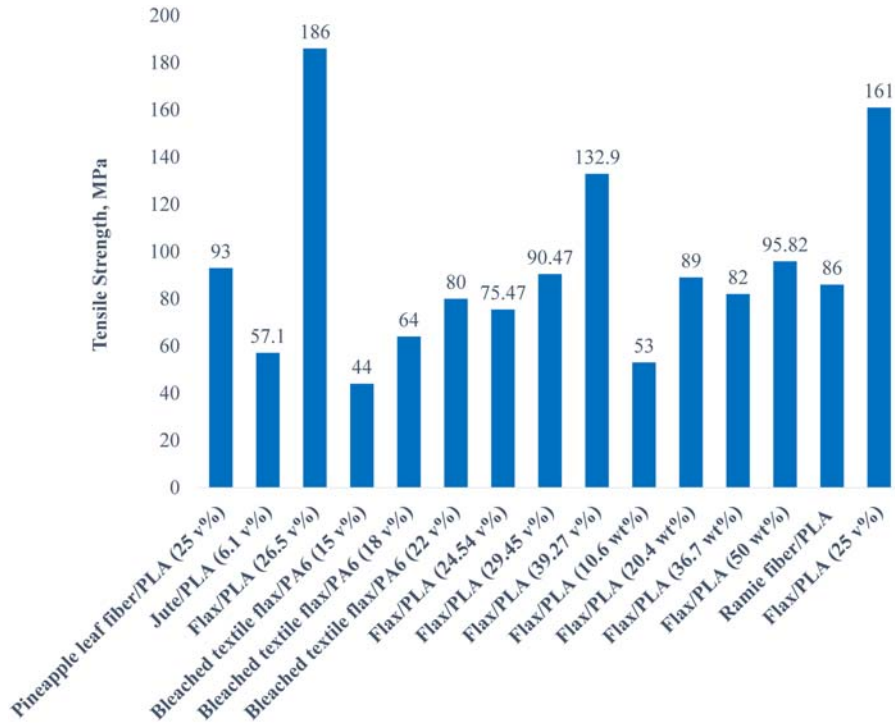

Figure 4.3 Comparative histogram of tensile strength of continuous UD natural fiber reinforced composites obtained by the FFF process for different fiber fraction (Zhang et al., 2020; Terekhina et al., 2022; Kuschmitz et al., 2021; Long et al., 2021; Yao et al., 2020; Matsuzaki et al., 2016; Suteja et al., 2020; Rivero-Romero et al., 2023; Cai, Wen, et al., 2022a; Cheng et al., 2021; Le Duigou, Chabaud, et al., 2020).

respectively) are in good accordance with the highest tensile properties of the FFF-printed UD flax/PLA composites (Marrot et al., 2014; Oksman, 2001; Coroller et al., 2013). Also, the average elastic properties of the FFF-printed UD flax/PLA composites are equivalent to those of UD hemp/PLA obtained by thermocompression molding for about the same fiber volume content ($V_f = 26\%$) (Baghaei et al., 2014), and their average maximum strength was even ~34% better. Regarding the UD flax/PA composites obtained using the composite FFF technique, there is approximately a 30% difference in tensile strength and modulus than those achieved through thermocompression molding, with the FFF-produced composites exhibiting roughly half the strength and modulus (Bourmaud et al., 2016). The fiber linear density as well as the fiber volume content have to be as high as possible to provide the best tensile properties, as the strength values of the plant fibers depend on their quality and variety. Therefore the average tensile properties of FFF-printed UD biocomposites remain more than twice as low as those obtained by conventional processes, primarily because of the high fiber tex and high fiber content usually used

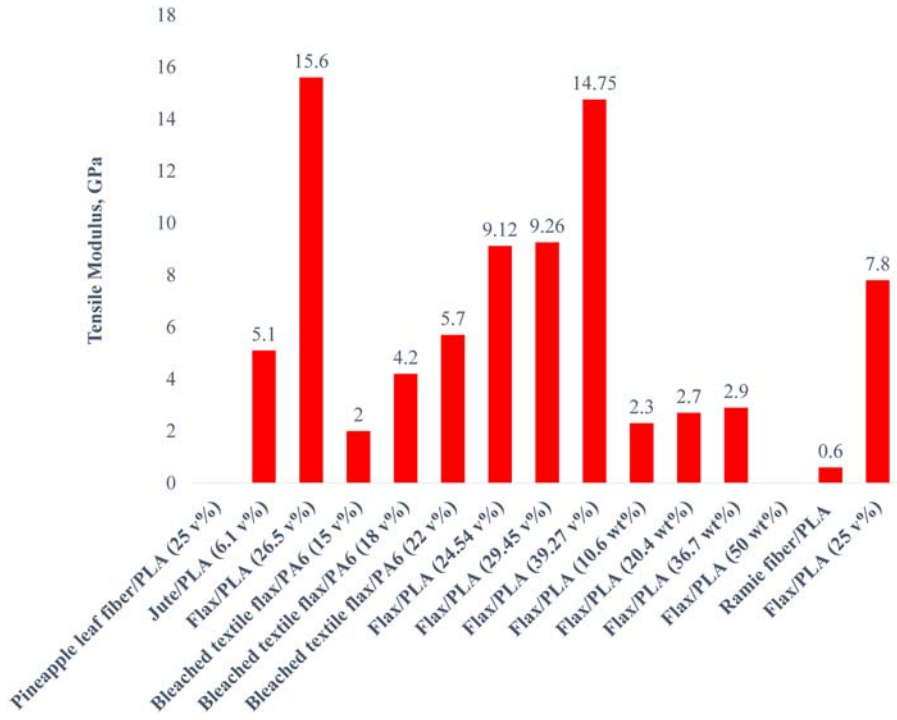

Figure 4.4 Comparative histogram of tensile modulus of continuous UD natural fiber-reinforced composites obtained by the FFF process for different fiber fraction (Zhang et al., 2020; Terekhina et al., 2022; Kuschmitz et al., 2021; Long et al., 2021; Yao et al., 2020; Matsuzaki et al., 2016; Suteja et al., 2020; Rivero-Romero et al., 2023; Cai, Wen, et al., 2022; Cheng et al., 2021; Le Duigou et al., 2020a).

for these processes (Shah, 2013; Bourmaud et al., 2016; Monti, 2016; Pantaloni et al., 2021; Couture et al., 2016). However, the FFF-printed UD Flax/PLA composites demonstrate a clear potential to be used in additive manufacturing as a replacement for other existing nonbiodegradable composite materials.

Fiber alignment, the absence of defects such as porosities, and the homogeneous distribution of the fibers in the matrix are key parameters in optimizing the composite tensile strength. However, the mechanical properties of FFF-printed plant-reinforced biocomposites are commonly lower than those reinforced with synthetic materials, which could be explained by the difficulties associated with printing them (Terekhina et al., 2022; Balla et al., 2019; Ahmed et al., 2020; Wang et al., 2018; Dey et al., 2021). Poor fiber/matrix adhesion, resulting from residual stresses caused by nonuniform temperature gradients (Terekhina et al., 2022; Matsuzaki et al., 2016; Agaliotis et al., 2022; Balla et al., 2019; Ahmed et al., 2020; Dey et al., 2021; Bi and Huang, 2022; Terekhina et al., 2020b), as well as chemical and surface incompatibilities between the fiber and the matrix (staircase effect) (Long et al., 2021; Ahmed et al., 2020; Wickramasinghe et al., 2020; Aida et al., 2021), crystallization

Table 4.1 Mechanical properties versus fiber fraction of different continuous unidirectional fiber reinforced bio-composites obtained by FFF (fused filament fabrication) extrusion techniques and conventional processes.

Type of continuous plant reinforcement	Type of TP polymer matrix	Fiber fraction	Manufacturing process	Mechanical properties	3D Printer	References
Pineapple leaf fiber	PLA	25 v%	In situ impregnation by FFF	Tensile strength: 90.04–96.78 MPa	ANET A8 3D Printer Prusa I3	Suteja et al. (2020)
Jute fiber (twisted 500-Tex double yarn)	PLA	6.1 v%	In situ impregnation by FFF	Tensile strength: 57.1 MPa Tensile Modulus: 5.1 GPa	Flash Forge printer	Matsuzaki et al. (2016)
Flax fiber (68 Tex)	PLA	26.5 v%	Filament extrusion by the FFF	Tensile strength: 186 ± 4 MPa Tensile Modulus: 15.6 ± 1.1 MPa	Prusa I3 printer	Le Duigou, Chabaud, et al. (2020)
Bleached textile flax fiber (39 Nm)	PA6	15 v% 18 v% 22 v% 15 v% 18 v% 22 v%	In situ impregnation by the FFF	Tensile strength: 44 ± 4 MPa 64 ± 3.5 MPa 80 ± 2.5 MPa Tensile Modulus: 2.0 ± 0.79 4.2 ± 0.6 5.7 ± 0.5	TEVO Black Widow	Terekhina et al. (2022)
Flax fiber (200 Tex)	PLA	24.54 v% 29.45 v% 39.27 v% 24.54 v% 29.45 v% 39.27 v% 24.54 v% 29.45 v% 39.27 v%	In situ co-extrusion by the FFF	Tensile strength: 75.47 ± 6.19 MPa 90.47 ± 0.83 MPa 132.90 ± 0.8 MPa Tensile Modulus: 9.12 ± 1.02 GPa 9.26 ± 0.58 GPa 14.75 ± 1.42 GPa Flexural strength: 77.72 ± 10.13 MPa 105.75 ± 3.09 MPa 130.99 ± 7.33 Mpa	Prusa I3 MK3S 3D printer	Kuschmitz et al. (2021)

(*Continued*)

Table 4.1 (Continued)

Type of continuous plant reinforcement	Type of TP polymer matrix	Fiber fraction	Manufacturing process	Mechanical properties	3D Printer	References
		24.54 v% 29.45 v% 39.27 v%		Flexural Modulus: 5.08 ± 0.74 GPa 7.88 ± 0.26 GPa 7.63 ± 3.04 GPa		
Flax fiber (68 Tex)	PLA	10.6 wt.% 20.4 wt.% 36.7 wt.% 10.6 wt.% 20.4 wt.% 36.7 wt.% 36.7 wt.% 36.7 wt.%	Filament extrusion by the FFF	Tensile Strength: 53 MPa 89 MPa 82 MPa Tensile Modulus: 2.3 GPa 2.7 GPa 2.9 GPa Flexural Strength: 132 MPa Flexural Modulus: 7 GPa	Atmega 2560 printer	Zhang et al. (2020)
Banana fibers	PLA	–	In situ impregnation by the FFF	–	Cartesian self-made printer	Rivero-Romero et al. (2023)
Flax fiber	PLA	50 wt.%, 9:7 v%	Filament extrusion by the FFF	Tensile strength: 95.82 MPa Flexural Strength: 79.84 MPa	Prusa I3	Yao et al. (2020)
Ramie fiber (36 Nm/2 R)	PP/EPDM/talc	–	In situ impregnation by the FFF	Flexural strength: 58 MPa Flexural Modulus: 3.6 GPa	Combot-200 printer	Cai, Wen, et al. (2022)
Ramie fiber (36 Nm/2 R)	PLA	–	In situ impregnation by the FFF	Tensile strength: 86 MPa Tensile Modulus: 0.6 GPa	Combot-200 printer	Cheng et al. (2021)

Flax fiber (67 tex)	PLA	25 v%	In situ impregnation by the FFF	Tensile strength: 161 MPa Tensile Modulus: 7.8 GPa Flexural strength: 111 MPa Flexural Modulus: 9 GPa	Yinke 235	Long et al. (2021)
Flax fiber (200 tex)	PP	35−40 v%	Liquid Resin Infusion	Tensile strength: 225 MPa Tensile Modulus: 23 GPa	–	Monti (2016)
Flax fiber (200 tex)	PA11	21 v% 28 v% 35 v%	Thermocompression molding	Tensile strength: 120 MPa Tensile Modulus: 12.2 GPa Tensile strength: 152 MPa Tensile Modulus: 15 GPa Tensile strength: 197 MPa Tensile Modulus: 19.4 GPa	–	Bourmaud et al. (2016)
Hemp fiber (0.415 tex)	PLA	26 v%	Thermocompression molding	Tensile strength: 73 MPa Tensile Modulus: 9 GPa	–	Baghaei et al. (2014)

(*Continued*)

Table 4.1 (Continued)

Type of continuous plant reinforcement	Type of TP polymer matrix	Fiber fraction	Manufacturing process	Mechanical properties	3D Printer	References
Flax fiber (100 tex)	PLA	50 wt.%	Thermocompression molding	Tensile strength: 106.3 MPa Tensile Modulus: 15.9 GPa Flexural strength: 140 MPa Flexural Modulus: 7.6 GPa	–	Gautreau et al. (2021)
Flax fiber (200 tex)	PLA	44.4 v%	Thermocompression molding	Tensile strength: 339 MPa Tensile Modulus: 20 GPa	–	Couture et al. (2016)
Flax fiber (100 gsm)	PLA	32 v%	Thermocompression molding	Tensile strength: 216 MPa Tensile Modulus: 20.1 GPa	–	Pantaloni et al. (2021)
Flax fiber (250 tex)	Bio epoxy Epoxy (petro) Epoxy (petro)	20 v% 32 v% 32 v%	Molding process RTM	Tensile strength: 130 MPa Tensile Modulus: 11.6 GPa Tensile strength: 224 MPa Tensile Modulus: 18.4 GPa Tensile strength: 132 MPa Tensile Modulus: 15 GPa	–	Marrot et al. (2014); Oksman (2001)

Flax fiber (250 tex)	Biopolyester Polyester (petro)	31 v% 28 v%	Molding process	Tensile strength: 174 MPa Tensile Modulus: 18.8 GPa Tensile strength: 185 MPa Tensile Modulus: 17.2 GPa	–	Marrot et al. (2014)
Flax fiber	Epoxy	22 v% 23 v% 36 v% 36 v%	Compression molding	Tensile strength: 208 MPa Tensile Modulus: 13 GPa Tensile strength: 165 MPa Tensile Modulus: 11 GPa Tensile strength: 207 MPa Tensile Modulus: 20 GPa Tensile strength: 271 MPa Tensile Modulus: 24 GPa	–	Coroller et al. (2013)

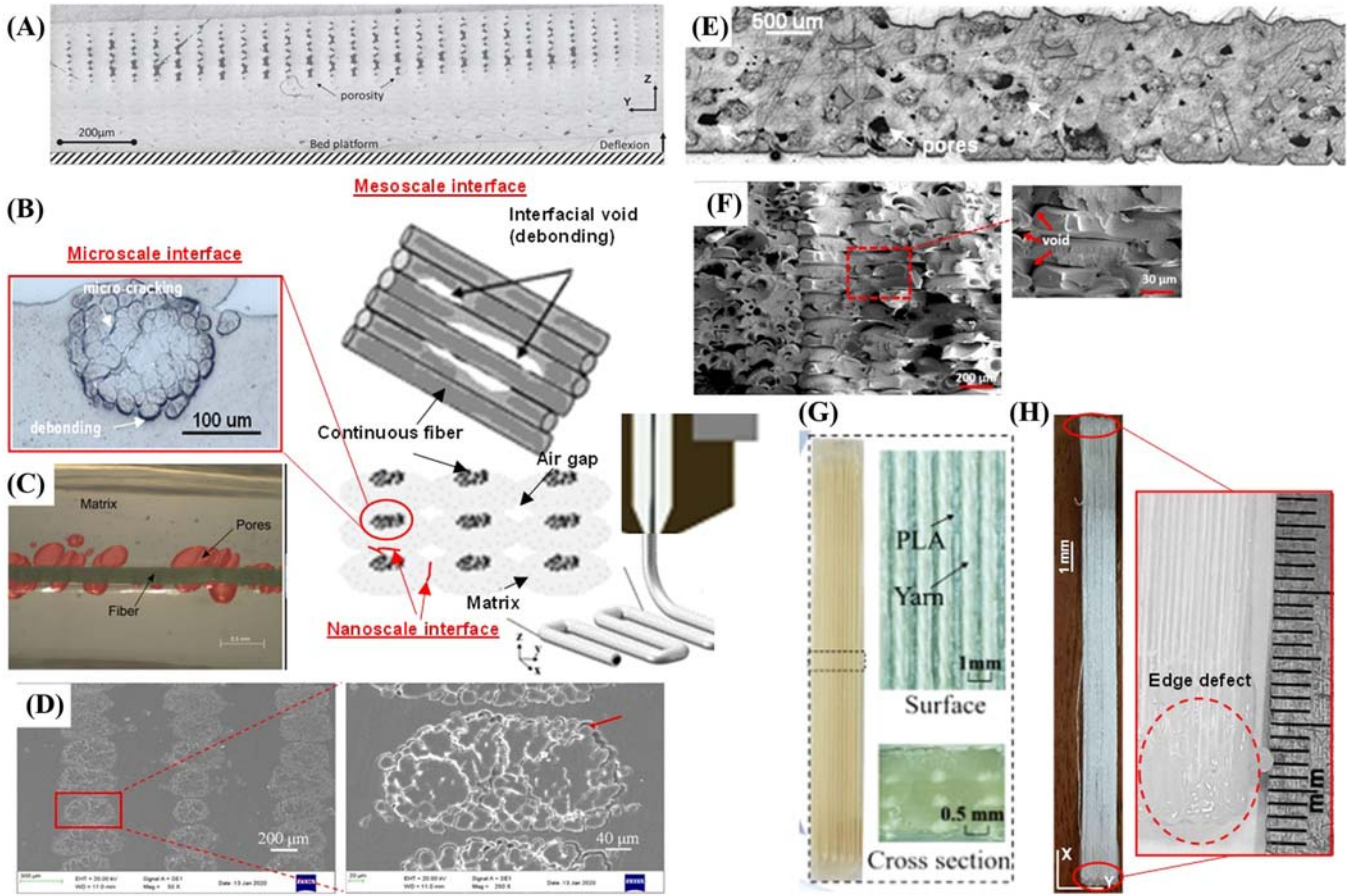

Figure 4.5 (A) Warping and pore formation due to crystallization of PA6 matrix (Terekhina et al., 2020b); (B) Schematic view of multiscale interfaces in the FFF printed bio-composite; (C) Microscale interface: voids (pores) at the fiber/matrix interface in the continuous banana

(*Continued*)

◀ reinforced composite (Rivero-Romero et al., 2023); (D) SEM images of cross-sectional views of untreated continuous flax/PLA (Long et al., 2021); Red arrows indicate interfacial voids; (E) Pores due to air gaps in the case of continuous flax/PA6 composite (Terekhina et al., 2022); (F) voids due to air gaps and interfacial debonding in the case of oil palm fiber/ABS composite (Ahmad et al., 2022); (G) Surface and cross-section aspect of continuous ramie yarn/PLA composite (Cheng et al., 2021); (H) Macroscopic defect at the edge of continuous flax/PA6 composite (Terekhina et al., 2022).

Source: From Terekhina, S., Tarasova, T., Egorov, S., Skornyakov, I., Guillaumat, L., & Hattali, M. L. (2020). The effect of build orientation on both flexural quasi-static and fatigue behaviors of filament deposited PA6 polymer. *International Journal of Fatigue*, *140*, 105825. https://doi.org/10.1016/j.ijfatigue.2020.105825; Rivero-Romero, O., Barrera-Fajardo, I., & Unfried-Silgado, J. (2023). Effects of printing parameters on fiber eccentricity and porosity level in a thermoplastic matrix composite reinforced with continuous banana fiber fabricated by FFF with in situ impregnation. *The International Journal of Advanced Manufacturing Technology*, *125*, 1893−1901. https://doi.org/10.1007/s00170-022-10799-8; Long, Y., Zhang, Z., Fu, K., & Li, Y. (2021). Efficient plant fiber yarn pre-treatment for 3D printed continuous flax fiber/poly(lactic) acid composites. *Composites Part B: Engineering*, *227*, 109389. https://doi.org/10.1016/j.compositesb.2021.109389; Terekhina, S., Egorov, S., Tarasova, T., Skornyakov, I., Guillaumat, L., & Hattali, M.L., 2022. In-nozzle impregnation of continuous textile flax fiber/polyamide 6 composite during FFF process. *Composites Part A: Applied Science and Manufacturing*, *153*, 106725. https://doi.org/10.1016/j.compositesa.2021.106725; Ahmad, M. N., Ishak, M. R., Taha, M. M., Mustapha, F., Leman, Z., Lukista, D. D. A., & Irianto and Ghazali I. (2022). Application of taguchi method to optimize the parameter of fused deposition modeling (FDM) using oil palm fiber reinforced thermoplastic composites. *Polymers*, *14*, 2140. https://doi.org/10.3390/polym14112140; Cheng, P., Wang, K., Chen, X., Wang, J., Peng, Y., Ahzi, S., & Chen, C. (2021). Interfacial and mechanical properties of continuous ramie fiber reinforced biocomposites fabricated by in-situ impregnated 3D printing. *Industrial Crops & Products*, *170*, 113760. https://doi.org/10.1016/j.indcrop.2021.113760.

of the polymer matrix (as seen in the case of PA6) (Terekhina et al., 2022; Balla et al., 2019; Terekhina et al., 2020b), and poor fiber distribution within the fiber-reinforced filament (Balla et al., 2019; Ahmed et al., 2020), contribute to the formation of different forms of porosity that negatively impact mechanical properties (Fig. 4.5A). Generally, these defects could be summarized as shape distortion and classified into three types of interfaces (Fig. 4.5B–F):

- **nanoscale interfaces** between two filling or weld lines (by forming the micro-voids or micro-pores). These voids could act as stressing concentration points and leads to sample failing, which consequently lead to inferior mechanical properties;
- **microscale interfaces** between the impregnated dry fiber yarn or towpreg (micro-cracking) and the polymer matrix, linked to poor polymer-fiber adhesion or wettability;
- **mesoscale interfaces** or air gaps formed between each filling line with potentially a lack of bonding (by forming the interfacial voids [or debonding]).

In addition, Fig. 4.5G,H shows a macroscopic defect observed at the edges of continuous plant fiber-reinforced composites, where the fiber does not follow the printing trajectory.

4.4 Solutions to enhance mechanical properties

Therefore, to increase the mechanical properties and overcome the print difficulties of these bio-composites, some solutions could be proposed:

- **Improvement of interfacial fiber/matrix adhesion**, by developing: (1) the quality of the yarn filament (linear density and twist angle variation, but also its variety) and realizing different surface fiber treatments (silane, alkali, acylation, benzoylation, malleated coupling agents, permanganate, acrylonitrile, and acetylation grafting, stearic acid, peroxide, isocyanate, triazine, fatty acid derivative sodium chloride, and fungi are examples of various types of chemical treatment that are available) (Long et al., 2021; Aida et al., 2021; Akil et al., 2011); and (2) fiber/polymer rheology, by controlling the evolution of crystallinity degree or adding the rheology modifier in the polymer matrix (Lee et al., 2021). Chemical pretreatments are generally used to modify and clean the fiber surface by increasing its roughness but also to reduce the moisture absorption process and upsurge the surface unevenness (Aida et al., 2021; Akil et al., 2011; Krishna and Kanny, 2016; Saba et al., 2015). Long et al. (2021) demonstrated the promising manufacturing quality of flax fibers treated with silane for in situ impregnation FFF process to obtain biocomposites with low void content and improved interfacial bonding and mechanical properties. The interlaminar fracture toughness increased by 11% and 23% for the two treated specimens, while their flexural properties improved by about +22.5% and +28% for flexural strength and modulus, respectively.
- **Control the printing pressure** before printing (Kuschmitz et al., 2021), during the process by developing the printer head with a compaction roller (Ueda et al., 2020) or local laser heating of interfacial layer (Ravi et al., 2016), and after the FFF process, by conducting posttreatments (ultrasonic welding, laser heating, annealing, and microwave heating) (Tran et al., 2022). The underlying mechanisms for these improvements are related to the enhancement of the interfacial bonding between layers/rasters, and the reduction of porosity by applying different external energy sources after the printing process;

- **Control the print velocity and rotation angle of fiber** at the corner/edge of the sample, using artificial intelligence (AI) to manage the retrofit loop to maintain the integrity of the printing trajectory.

4.5 Effects of processing parameters

The FDM/FFF 3D manufacturing process is influenced by numerous parameters, all of which must be carefully controlled and defined to obtain optimum mechanical properties, dimensional accuracy, surface roughness, or cost. Consequently, selecting which parameters to prioritize over others is a challenging decision. Usually, operators choose from these parameters based on their experience and acquired knowledge. In the most commonly used thermoplastic polymers, such as PLA, ABS (acrylonitrile butadiene styrene), and PA6, numerous studies and recommendations in the form of manuals or webpages have investigated the effects of potential parameters on the mechanical and fatigue properties of 3D-printed parts (Terekhina, et al., 2021; Terekhina et al., 2020a,b; Auffray et al., 2022). While these parameters may be well controlled and understood in thermoplastic polymers, the same cannot be said for CNFRCs. Because of the limited literature on the effect of these parameters on CNFRC filaments, this section outlines the main adjustable parameters used in the FDM/FFF 3D process and their influence on mechanical and physical properties. As observed in Fig. 4.6, the exploration of the mechanical properties of samples obtained through the FDM/FFF process is less tackled in the case of CNFRCs.

Printing speed, nozzle temperature, layer height, hatch spacing, and filament flow rate are all critical factors that influence mechanical properties. The critical

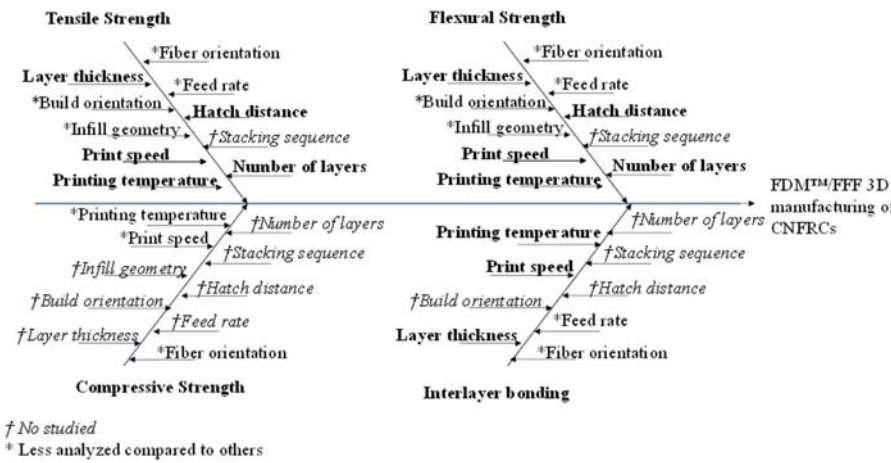

Figure 4.6 A fishbone diagram to illustrate the main effect of process parameters on the 3D CNFRCs obtained by FDM/FFF processes. *CNFRCs*, continuous natural fiber reinforced composites; *FDM*, fused deposition modeling; *FFF*, Fused filament fabrication.

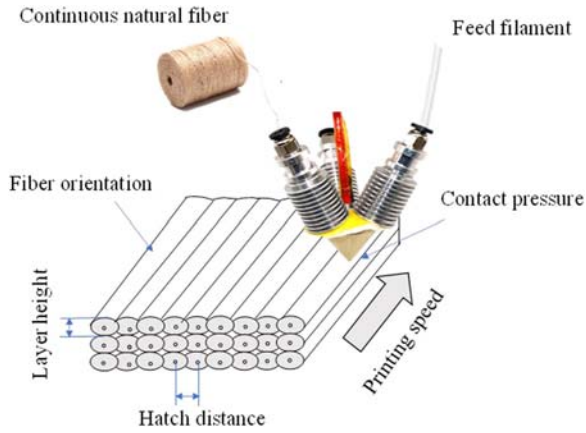

Figure 4.7 Main printing parameters that influence the mechanical properties of CNFRCs. *CNFRCs*, continuous natural fiber reinforced composites.

factors influencing mechanical properties are represented in Fig. 4.7. The effects are discussed in the following subsections. However, some process parameters, such as build orientation, infill geometry, feed rate, and stacking sequence, need to be analyzed or studied.

4.5.1 Printing speed

Printing speed is defined as the nozzle's speed of travel during the deposition process in the X-Y plane. It affects the part strength, dimensional accuracy, surface quality, and manufacturing time (Rajendran Royan et al., 2021; Auffray et al., 2022; Tian et al., 2022). Generally, printing speeds for neat polymers rarely exceed 4000 mm/min, while in the case of CNFRCs, it is less than 1000 mm/min and depends on the technology used (see § 4.2). It was observed that at high printing speeds, the interfacial bonding between deposited filaments is limited, resulting in poor interlayer adhesion and porosity. For CNFRCs, high printing speed shortens the fiber-matrix impregnation time, resulting in both poor fiber-matrix and interlayer bonding, which can increase porosity density (Cheng et al., 2021; Tekinalp et al., 2014). Consequently, as printing speed rises, tensile, flexural, and shear properties slightly decrease, but the effect is minor (Zhang et al., 2018; Christiyan et al., 2016; Tian et al., 2016). Cai, Wen, et al. (2022), in their study on 3D-printed continuous ramie fiber reinforced polypropylene (CRFRPP) composites, found that when the printing temperature was 190°C, the interlayer and intralayer strength increased with the increase in printing speed from 100 to 500 mm/min. However, when the printing temperature is between 210°C and 230°C, the printing speed has an insignificant effect on the interlayer and intralayer strength. Rivero-Romero et al. (2023) studied the effect of printing speed on the formation of porosity for continuous banana fiber/PLA composites. Their results show that the porosity

fraction is affected by the staying time of fiber in the printing head during the process. When the printing speed decreases, the impregnation time of banana fiber increases, allowing it to decrease the dynamic contact angle on the fiber surface. From 180 to 321 mm/min, the porosity level decreases from 9.5% to 0.63%, respectively. The printing speed also affects the dimensional accuracy of a part. A low printing speed prevents vibration of the nozzle, so the deposited filament is steadily positioned on top of the previous layer, allowing for more ordered filament and higher accuracy (Lanzotti et al., 2015). To ensure strong adhesion between the part and the printing bed in certain Slicer (G-code generator) software, the printing speed of the first layer, which is in contact with the printing bed, is set lower than the subsequent layers. This strategy is explained by the fact that a slower printing speed increases the time for material compaction, allowing the nozzle to apply pressure more effectively.

4.5.2 Nozzle temperature

This is the material extrusion temperature and is a significant parameter in composite manufacturing because it influences both the impregnation of reinforcing fibers and the chemical structure of polymer matrices. Cai, Wen, et al. (2022) considered that the contribution of printing temperature in interbonding strength is about 32%. A high temperature causes the filament to be less viscous, consequently bonds better to the previously deposited layer, and significantly reduces the voids, enhancing the mechanical property (Cheng et al., 2021; Kabir et al., 2020). When dealing with CNFRCs, certain fibers have low thermal stability and can only handle temperatures below 210°C, which implies a limited use of materials (Terekhina et al., 2022; Le Guen et al., 2019; Badouard et al., 2019). A temperature above 210°C tends to degrade lignocellulosics in natural fiber, which could result in negative effects on the mechanical properties. For this reason, typical printing materials cited in the literature are PLA and ABS. Terekhina et al. (2022) have succeeded in overcoming the temperature limit in the PA6/flax fiber composite by reducing the residence time of flax fiber in the nozzle and, thus, preventing its degradation. From another perspective, a high nozzle temperature increases the crystallinity of some semicrystalline polymer filaments, such as polypropylene and polyethylene. Although it allows to increase the tensile strength, the crystallinity induces severe shrinkage and warpage during part cooling, which explains why some polymers are less studied than others (Terekhina et al., 2020b; Krajangsawasdi et al., 2021). As a result, printed composites lose their esthetic characteristics and dimensional precision with some semicrystalline polymers. A temperature should be chosen that preserves the part's appearance and dimensional accuracy while still providing acceptable mechanical characteristics.

4.5.3 Material feed rate or flow rate

The feed rate is the velocity at which the solid filament material is extruded. This velocity controls the amount of materials in the heated nozzle that controls the

pressure drop and reduction pressure along the convergence printing nozzle, following Bernoulli's principle. Theoretically, the feed rate (F_R) can be calculated from the material flow rate (Q) and the expected dimension of the printed filament (width (w) and height (h)) or the angular velocity of the feeder motor (ω) and the feeder roller radius (R_f) using Eq. (4.1):

$$F_R = \frac{Q}{wh} = \omega R_f \tag{4.1}$$

There are very few studies on the impact of material feed rate on CNFRC materials. Almost all studies have been carried out on carbon and glass fibers (Krajangsawasdi et al., 2021). It has been reported that a high feed rate, over 80 mm/min, may cause an excessive melting pressure that induces a melt flow upward along the gap between the nozzle wall and the convergence zone in the nozzle, thereby blocking the nozzle (Yao et al., 2020). Cai, Wen, et al. (2022) show that the interaction between printing temperature and printing speed is obvious. When the extrusion flow rate was low, with increasing printing temperature, the interlayer and intralayer strength of CRFRPP composites were significantly improved. However, when the extrusion flow rate was high, CRFRPP with a moderate printing temperature also had high interlayer and intralayer strength. Suteja et al. (2020) showed that the feed rate had a significant effect on the tensile strength and elongation of the pineapple leaf fiber reinforced PLA composite parts. Specifically, increasing the feed rate led to an increase in tensile strength. In practice, there exists a crucial relationship between the print speed (Ps) and feed rate (F_R), which users must adhere to, particularly in the separate fiber and matrix printing system (in situ impregnation) (see § 4.2), to prevent unstable dimensions in the printed part and to control the fiber content:

$$\frac{Ps}{F_R} = \left(\frac{D}{d}\right)^2 \tag{4.2}$$

Where d is the diameter of the nozzle and D is the solid filament diameter (Krajangsawasdi et al., 2021). The relation leads to underscoring the importance of nozzle diameter and geometry. Typically, the nozzle diameters available for commercial neat thermoplastic 3D printing filament range from 0.1 to 0.6 mm, depending on the accuracy required for the printed part. For the CNFRCs, the nozzle diameter ranges from 0.6 to 1.5 mm (Terekhina et al., 2022; Le Duigou et al., 2020). Terekhina et al. (2022) have machined a specific convergent nozzle, permitting the introduction of a continuous twisted yarn and polyamide 6 (PA6) filament via two separate channels, followed by mixing in the small heated zone (linear distance of 2 mm) before extruding from a conic flat-head nozzle. The flat-head nozzle is expected to compact and compress the composite filament to reduce voids. Markforged uses a convergent nozzle diameter of 0.9 mm with a filleted outlet edge for their continuous fiber reinforced nylon filament. The filleted outlet edge serves to guide the continuous fiber and facilitate its placement on the bed (MarkForged, 2023). The nozzle diameter (d) is also linked to the fabrication time,

which is calculated based on feed rate (F_R), part volume (V), and total layer height ($\sum \Delta h$) using Eq. (4.3).

$$t = \frac{V}{(dF_R \sum \Delta h)} \tag{4.3}$$

4.5.4 Layer height

Layer height (Δh) refers to the thickness of one layer of material deposited. For neat polymers, it has been shown that the lower layer height increases the mechanical strength through two mechanisms:

- First, it decreases the gaps between extruded filaments at adjacent layers, resulting in a less porous structure and higher stiffness.
- Second, the contact area between the extruded filaments increases, favoring heat transmission between layers and enhancing layer adhesion (Bakhtiari et al., 2023).

For CNFRCs, the same behavior is observed. Cheng et al. (2021) studied the interfacial and mechanical properties of continuous ramie fiber reinforced composites (CRFRCs)/PLA bio-composites. The authors reported that the highest tensile strength was obtained with the smallest layer height of 0.3 mm and noted that the printer layer of 0.2 mm led to easy breakage of the continuous ramie yarn caused by friction between the nozzle and the deposited filament. Moreover for a layer height greater than or equal to 0.7 mm, the process induces the delamination of the layers. The lower layer thickness provides good packing density and high interbonding strength, leading to high interfacial properties (Cheng et al., 2021; Kabir et al., 2020; Le Duigou et al., 2020; Tian et al., 2016). Although many available FDM/FFF printers can achieve layer heights of up to 0.05 mm, it is not at all practical when using continuous natural fiber filaments. The current reported values for the layer height range from 0.2 to 0.6 mm, whereas the nozzle diameters are between 0.6 and 1.5 mm (Terekhina et al., 2022; Cai, Wen, et al., 2022; Cheng et al., 2021; Le Duigou et al., 2020).

4.5.5 Hatch distance

Hatch distance (H) is the central distance between two adjacent deposited filaments. Tian et al. (2016) are among the first to study the effect of this parameter on the mechanical properties of 3D-printing parts. The authors have shown that increasing hatch distance from 0.4 to 1.8 mm (for a nozzle diameter of 2 mm) results in a significant reduction in the flexural properties of continuous carbon fiber/PLA composites. The hatch distance and layer height play an important role in the fiber volume ratio (V_f) calculation. Cai, Lin, et al. (2022) investigated the effect of hatch distance on the dynamic strength of 3D-printed CRFRCs. The results showed that hatch distance had a nonlinear and interactive influence on the dynamic strength of CRFRCs. Specifically, decreasing the hatch distance and layer height led to an

increase in the impact strength of the printed bio-composites. Terekhina et al. (2022) in their study on continuous flax fiber/PA6 composites estimate the fiber volume ratio in two ways, theoretically (V_{f_th}) using Eq. (4.4) and experimentally (V_{f_exp}), assuming porosity content as zero using Eq. (4.5).

$$V_{f\_th} = \frac{S_f}{S_c} = \frac{\pi r_f^2 N_f N}{ab} \tag{4.4}$$

$$V_{f\_exp} = \frac{1}{\frac{\rho_f}{\rho_m}\left(\frac{1}{\tau_m^f} - 1\right) + 1} \tag{4.5}$$

where S_f and S_c are the section area of flax yarns and composites, respectively; r_f is the radius of flax yarn; N_f is the number of flax yarns in the ply; N is the number of plies in the composite; a and b are the cross-section dimensions of the composite; ρ_f, ρ_m are the densities of fiber and polymeric matrix, respectively; and τ_m^f is the fiber mass ratio, estimated by:

$$\tau_m^f = \frac{N tex_f L_f}{m_c} \tag{4.6}$$

where tex_f is the linear density (g/1000 m) of flax yarns; L_f is the length (m) of flax yarns that is used to infill the composite's surface ply; m_c is the mass of the composite.

Their results demonstrate that the higher the value of H, the lower and, consequently, the poorer the mechanical properties are (Table 4.2). However, there is an optimum where H should be neither too far apart nor too close together to obtain the best mechanical strength. Spacing the fibers too close together prevents better impregnation of the fibers by the matrix and, consequently, better mechanical properties. The same results have been obtained by Cai, Wen, et al. (2022).

4.6 Reinforcement geometry and orientation

Continuous fiber reinforced polymer composites (CFRPCs) fully combine the advantages of low material density and strong structural designability and are widely used in automobiles, aircraft, and space. However, conventional processes often involve expensive mold requirements and challenges in fabricating complex-shaped lightweight structures, which limit the application and development of CFRPC. Compared with conventional manufacturing processes, 3D-printed continuous fiber reinforced composites provide a new low-cost rapid fabrication method and more freedom for the individual design of CFRPCs. Fig. 4.8 represents the trend of the number of published articles on 3D CFRPCs.

It can be found that most published articles were focused on the 3D printing of continuous synthetic fibers reinforced composites due to their broad use in the composite manufacturing field. However, with the increase in global ecological and

Table 4.2 Effect of height layer (Δh) and hatch distances (H) on mechanical properties of flax fiber/PLA composites.

Authors and material	⌀, mm	FFF process techniques	H, mm	Δh, mm	Stacking orientation	V_f (%)	V_p	E_L, GPa	σ, MPa
Flax fiber/PA6 (26 Tex, 39 Nm, Safilin)	0.6	In situ impregnation	0.4	0.2	$[0]_5$	22	4 ± 1	5.7 ± 0.5	82 ± 2.5
			0.55	0.2	$[0]_5$	18	5 ± 0.5	4.2 ± 0.6	66 ± 3.5
Terekhina et al. (2022)									
Flax fiber/PLA (68 Tex, Safilin)	0.6	Filament extrusion	0.4	0.3	$[0]_1$	26.5	5.4 ± 0.8	12.9 ± 0.9	135 ± 10
Le Duigou et al. (2019, 2020)			0.6	0.3	$[0]_1$	26.5	3.2 ± 0.7	15.6 ± 1.1	186 ± 4
			0.8	0.3	$[0]_1$	26.5	2.3 ± 0.9	17.1 ± 1.5	147 ± 16
			0.6	0.25	$[0]_1$	30.4	3.2 ± 0.7	23.3 ± 1.8	253.7 ± 15
Flax fiber/PLA	1	In situ co extrusion	–	0.66	$[0]_5$	24.54	–	9.12 ± 1.02	75.47 ± 6.19
(200 Tex, Tönisvrost)			–	0.66	$[0]_6$	29.45	–	9.26 ± 0.58	90.47 ± 0.83
Kuschmitz et al. (2021)			–	0.51	$[0]_8$	39.27	–	14.75 ± 1.42	132.9 ± 0.8

⌀: nozzle diameter, V_f: volume fraction rate, V_p: porosity content, E_L: longitudinal tensile modulus, σ: tensile strength.

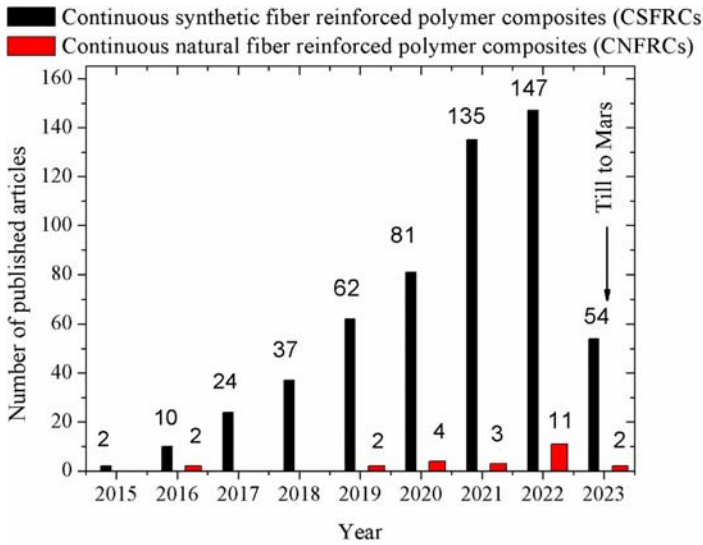

Figure 4.8 Number of published articles regarding CFRPC (data obtained from the Web of Sciences from 2015 to April 2023 using keywords: 3D printing, continuous fiber reinforcement, composites). *CNFRCs*, continuous natural fiber reinforced composites.

environmental pollution problems, these synthetic fiber reinforcements cannot meet today's environmental aims and sustainable development requirements. Under these circumstances, the manufacturing of continuous natural fiber reinforcement filled with biodegradable and recyclable polymer composites via 3D printing started to receive attention. Like printing parameters, reinforcement geometry and fiber orientations are both critical parameters that influence mechanical qualities.

4.6.1 Fiber orientations

The fiber orientation is related to the filament orientation deposition on an X-Y plane (horizontal axis of the machine). The X-axis is parallel to the tensile load direction, referred to as the low orientation angle [0 degree], and the Y-axis is perpendicular to the load direction, referred to as the high orientation angle [90 degree]. Typically, the optimal condition would be to have the fiber angle match the direction of loading. In this context, several authors have studied the effect of natural continuous fiber orientation ([0 degree], [± 45 degree], and [90 degree]) on the tensile and flexural properties (Terekhina et al., 2022; Le Duigou et al., 2019; Suteja et al., 2020; Ahmad et al., 2022). Unsurprisingly, Terekhina et al. (2022) found that the [0 degree] orientation exhibited better mechanical performance, that is, higher tensile strength and stiffness compared with the [90 degree] and [± 45 degree] orientations. This behavior is attributed to the fact that these orientations do not or partially support the axial loading during the tensile tests. It is important to note that in all considered fiber orientations, matrix filament cracking and interlayer

delamination, followed by fiber pull-out attributed to fracture, are observed. Based on the assumption that the mechanical strength of fiber-reinforced polymers is highest in the direction of fiber alignment, Zhang et al. (2020) tried to ensure that continuous fibers were arranged along the direction of the force gradient using a 3D FFF five-axis machine. The build orientation was divided into three types: upright, flat, and curved. These results show that flax fiber laying along the curvature direction could effectively improve the bending performance compared with neat PLA samples. Cheng et al. (2021) evaluated the effect of 3D-printed architecture on the penetration property of ramie fiber/PLA composites. The woven-like and nonwoven-like ramie fiber reinforcement bio-composites with different lay-up configurations were designed and fabricated (unidirectional layup, orthogonal layup, and woven-like layup). Their results show that the bio-composites formed in the woven-like architecture presented much higher energy absorption and maximum penetration force than those for the nonwoven-like bio-composites. It is important to note that the presence of orthotropic interweaved and undulated yarns in the woven-like architecture led to the prevention of fiber damage onset and deflection of the crack propagation path.

4.6.2 Reinforcement geometry

The 3D printing of cellular or lattice structures is almost exclusively applied to metallic, polymeric, and ceramic materials. Current research tries to copy and extend these structures for composite materials. To date, most of the published studies have focused on synthetic continuous fiber-reinforced composites, and some timid approaches have been taken in the CNFRCs. Fruleux et al. (2022) evidenced the difference between programmed tool path geometry and the resulting shape of the printed sample made with natural continuous flax fiber/PLA. Three geometries were studied: circular, star, and octagonal shapes (Fig. 4.9A). For a circle shape with a diameter between 20 and 30 mm, the printing fidelity is at its maximum, between 70% and 80% of the targeted programmed area. They suggest that when designing cellular materials, the use of natural continuous flax fiber with PLA may be limited to an internal diameter of 15 mm. For diameters less than 15 mm, accurate experimental quantification of the area becomes challenging. For star and octagonal shapes, they observe a relatively high printing fidelity between programmed angle and printing geometry for angles greater than 60 degrees ($>90\%$), whereas below this value, a large discrepancy exists between the target toolpath geometry and the measurements. Zhang et al. (2020) printed a leaf spring part and shoe cap made of continuous fiber flax reinforced PLA using a five-axis 3D printing machine (Fig. 4.9B). The average density of printed parts was around 1.167 g/cm^3. They demonstrate that the use of CNFRCs on functional parts will have far-reaching significance in composite fabrication, where the current demand is for low-weight and high-performance parts.

For synthetic continuous fibers reinforced composites, some published articles came to study the complex-shaped lightweight structures considering grid, truss, corrugated, or lattice structures (Rajendran Royan et al., 2021; Sugiyama et al., 2018). Sugiyama et al. (2018) obtained a 3D printing sandwich structure by printing the skin

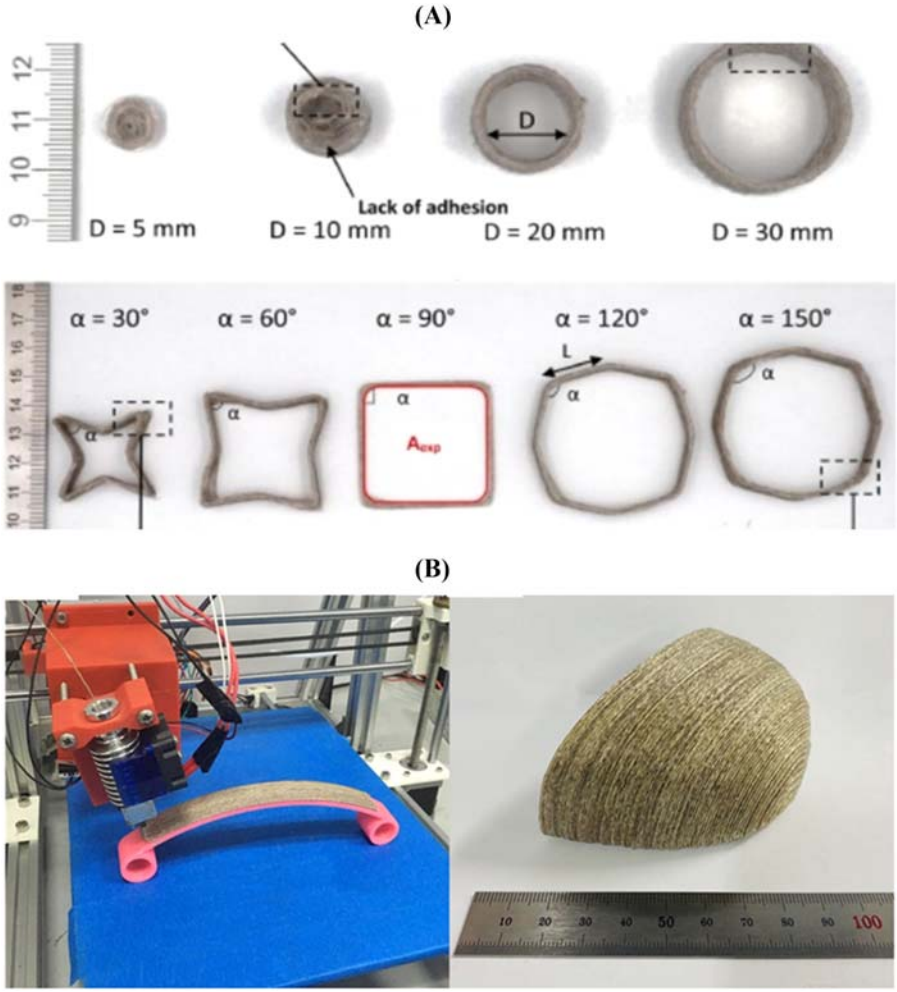

Figure 4.9 3D printing of CNFRCs: (A) Circular, star, and octagonal shapes (Fruleux et al., 2022), and (B) Component fabricated by five-axis 3D printing machine: Leaf spring (left), Shoe cap (right) (Zhang et al., 2020).
Source: From Fruleux, T., Castro, M., Correa, D., Wang, K., Matsuzaki, R. & Duigou, A. L. (2022). Geometric limitations of 3D printed continuous flax-fiber reinforced biocomposites cellular lattice structures. *Composites Part C: Open Access, 9*. https://doi.org/10.1016/j.jcomc.2022.100313; Zhang, H., Liu, D., Huang, T., Hu, Q., & Lammer, H. (2020). Three-dimensional printing of continuous flax fiber-reinforced thermoplastic composites by five-axis machine. *Materials 13*, 1678. https://doi.org/10.3390/ma13071678.

structure directly on the grid core. Various core structures were printed successfully: honeycomb, rectangle, grid, circle, and rhombus (Fig. 4.10) (Sugiyama et al., 2018; Hao et al., 2018; Liu et al., 2018; Eichenhofer et al., 2017; Hou et al., 2018). Liu et al. (2018) proposed a free-hanging 3D printing method for processing continuous

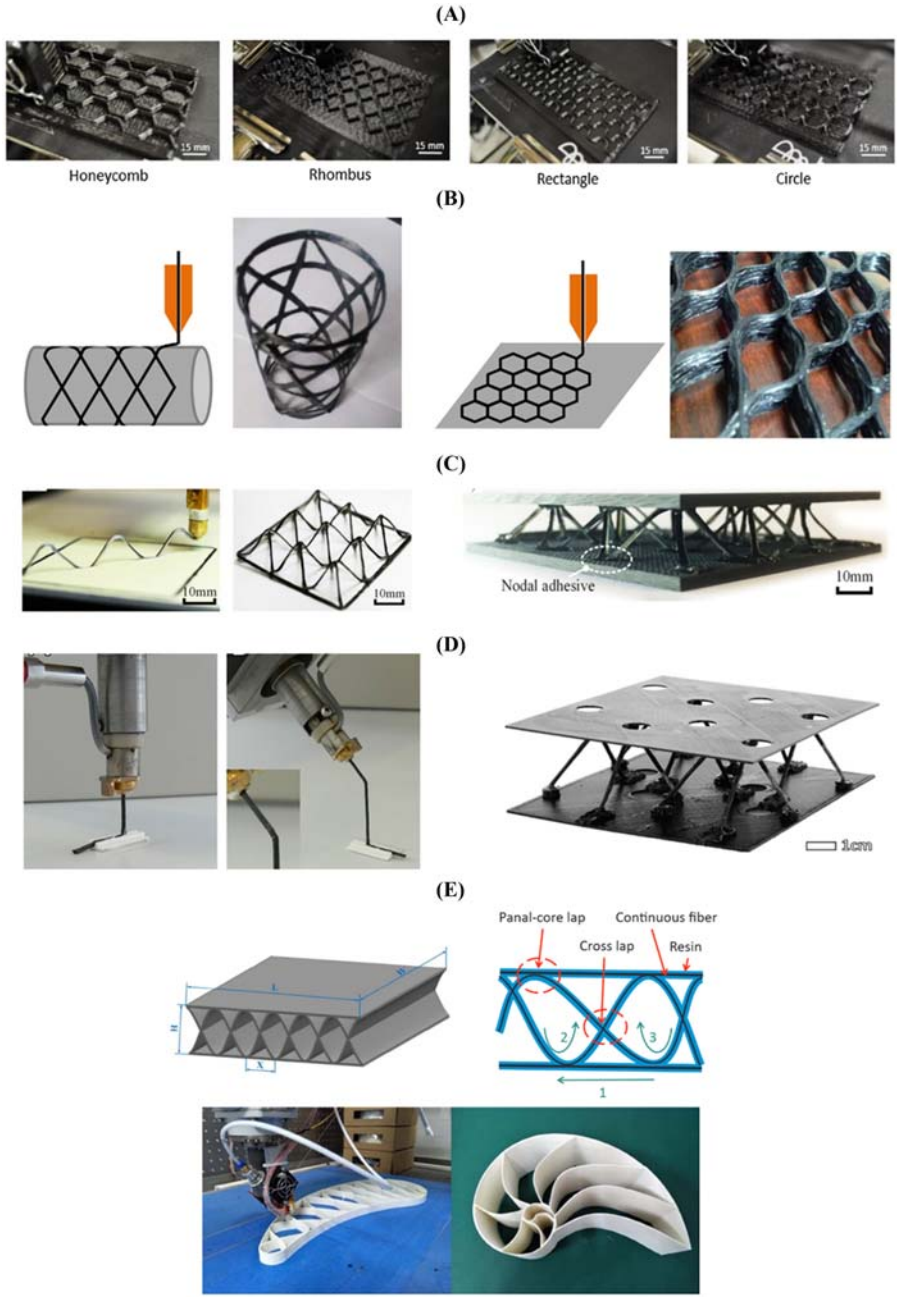

Figure 4.10 3D printing of CFRLSs: (A,B) Grid structures (Sugiyama et al., 2018; Hao et al., 2018), (C,D) Truss structures (Liu et al., 2018; Eichenhofer et al., 2017); (E) Corrugated structures (Hou et al., 2018).

(*Continued*)

fiber-reinforced thermoplastic lattice structures. The printing path generation was determined based on the relationship between printing constraints and parameters. This approach enabled the successful accomplishment of the unsupported 3D printing of the truss core through path design based on the enhancement of material stiffness by continuous fibers, proving the feasibility of continuous fiber suspension printing (Fig. 4.10C). Eichenhofer et al. (2017) introduced a process, called continuous lattice fabrication for the direct formation of composites along desired trajectories, including the z-direction. The feasibility of the process was shown by printing primary and secondary structures onto a plastic substrate, as well as by further showcasing the potential in the fabrication of an ultra-lightweight sandwich panel with a core density of 9 mg/cm^3 (Fig. 4.10D). Hou et al. (2018) proposed a cross-lap and panel-core lap design to fabricate composite fiber reinforcement lightweight structures (CFRLSs) with a complex shape and low cost. The effects of process parameters and printing paths on fiber distribution and structural properties are studied (Fig. 4.10E). Results show that the fiber content, structure configuration, and density of lightweight structures of CFRLSs can be adjusted through process parameters and printing path design, which greatly expands the design space of CFRLSs. To the best of the authors' knowledge, none of the approaches cited above have been developed or implemented to fabricate fully 3D structures based on CNFRCs. Although the development of these approaches will have significance for composites.

Current research is shifting toward 4D printing materials, origami structures, kirigami structures, or smart materials (Le Duigou et al., 2020) (Fig. 4.11). These materials have complex structures with original properties and are often composed of periodic or nonperiodic cell patterns. For example, Le Duigou et al. (2020) used wood activation techniques to print either wood-only or wood-based multimaterials. Folding through differentiated wood printing has been achieved through the control of the density and pattern of the printed wood (Fig. 4.11A). For example, for one curling deformation, all the expansion due to the anisotropic orientation of the fiber is directed along one axis. To obtain both curling and twisting deformation angles, a specific printing pattern of filament is printed (Fig. 4.11B).

◀ *Source:* From Sugiyama, K., Matsuzaki, R., Ueda, M., Todoroki, A. & Hirano, Y. (2018). 3D printing of composite sandwich structures using continuous carbon fiber and fiber tension. *Composites Part A: Applied Science and Manufacturing*, *113*, 114−121. https://doi.org/10.1016/j.compositesa.2018.07.029; Hao, W., Liu, Y., Zhou, H., Chen, H., & Fang, D. (2018). Preparation and characterization of 3D printed continuous carbon fiber reinforced thermosetting composites. *Polymer Testing*, *65*, 29−34. https://doi.org/10.1016/j.polymertesting.2017.11.004; Liu, S., Li, Y., & Li, N. (2018). A novel free-hanging 3D printing method for continuous carbon fiber reinforced thermoplastic lattice truss core structures. *Materials & Design*, *137*, 235−244. https://doi.org/10.1016/j.matdes.2017.10.007; Eichenhofer, M., Wong, J.C.H., & Ermanni, P. (2017). Continuous lattice fabrication of ultra-lightweight composite structures. *Additive Manufacturing*, *18*, 48−57. https://doi.org/10.1016/j.addma.2017.08.013; Hou, Z., Tian, X., Zhang, J., & Li, D. (2018). 3D printed continuous fiber reinforced composite corrugated structure. *Composite Structures*, *184*, 1005−1010. https://doi.org/10.1016/j.compstruct.2017.10.080.

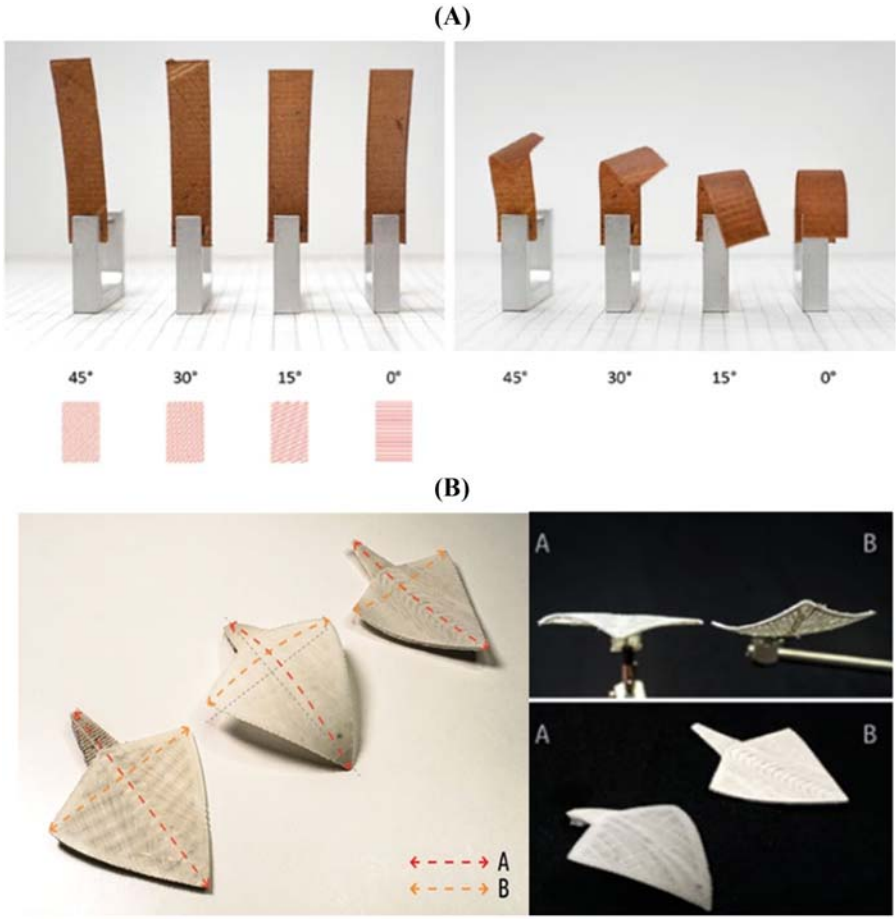

Figure 4.11 4D-printing composite material using natural fiber. (A) Controlled curling angles based on 3D-printed wood: effect of printing orientation on the response to different RH, (B) A specific printing pattern with a paraboloid distribution of wood filament induced double curvature (Le Duigou et al., 2020).
Source: From Le Duigou, A., Correa, D., Ueda, M., Matsuzaki, R., & Castro, M. (2020). A review of 3D and 4D printing of natural fiber biocomposites. *Materials & Design 194*, 108911. https://doi.org/10.1016/j.matdes.2020.108911.

4.7 Future trends and applications

To reduce environmental pollution, it is inevitable to turn toward biodegradable plant-reinforced composites. Some perspectives of FFF-printed CNFRCs were recently discussed in several contributions (Lee et al., 2021; Balla et al., 2019; Ahmed et al., 2020; Bhagia et al., 2021; Wang et al., 2018; Dey et al., 2021;

Bi and Huang, 2022; Aida et al., 2021; Shahrubudin et al., 2019; Quan et al., 2020). The following future trends can be highlighted:

- In terms of sustainability, CNFRCs will undergo treatment to enhance their mechanical properties while adhering to recycling and remanufacturing approaches for the production of fully recyclable green composites.
- FFF technology will lead to a change in the structural concept through the fabrication of lightweight bio-composite structures tailored for well-defined applications. Although most published studies have focused on continuous synthetic reinforced composite materials: pyramide, spring, grid (Sugiyama et al., 2018), truss (Liu et al., 2018), auxetic honeycomb (Quan et al., 2020), and corrugated structures (Hou et al., 2018), this list is by no means exhaustive. The availability of lightweight structures with excellent energy absorption is essential for numerous engineering applications, from the packaging to front structures of cars, trains, and building structures. In nature, plants and animals offer many excellent properties with low density, high strength, and energy absorption capacities that inspire us (Wegst et al., 2015). Bio-inspiration will boost the further development of continuous plant-reinforced bio-composite structures where the need to print the continuous fiber in the Z-printing direction (z-pinning), such as 3D lattice, coupled with complex geometry shape, is highly prevalent.
- FFF will further involve multimaterial printing by combining CNFRCs with other materials (mixing with carbon reinforcement or using shape memory polymers as the matrix). This integration opens the way for novel functionalities, such as shape-morphing composite structures or 4D printing, expanding the potential applications of FFF technology. Four-dimensional printing combines the AM technique with printable smart materials to allow the shape or properties of the printed structure to change over time under exposure to external stimuli (as a combination of temperature/moisture stimuli in the case of plant fiber-reinforced composites).
- To facilitate, optimize, and fasten the FFF process, machine learning, and artificial intelligence will be commonly used to select the best set of printing variables, and material design will be facilitated by the utilization of cloud computing (Cai, Wen, et al., 2022; Lu et al., 2023).

In the past decades, plant fiber-based composite applications obtained by conventional processes have become popular. The current global trend of biodegradability, eco-friendliness, faster processing time, lower cost, lightweight, high specific strength, and recyclability has led to an increase in industrial production. As a result, plant fiber composites are increasingly being used in many industries, including automobiles (e.g., bumpers, brake lining, parking brake lever, floor coverings, spare tire covers, interiors, and clutches), construction, ballistics, aircraft components, food packaging, sports equipment, electrical components, and biomedical materials (Akter et al., 2023). FFF could therefore be essential in revitalizing the cited applications, allowing for the creation of lighter and more complex structures within shorter timeframes. However, natural fiber-reinforced polymer composite in additive manufacturing is still in its infancy, and it cannot be denied that it has gained a lot of attention and favor in both industry and academia in recent years. Nonetheless, there are already many concrete end-use products made of continuous carbon-reinforced composites (CCFRCs) by additive manufacturing:

- Aerospace industry: Unmanned aircraft (3D printed CCFRC structure for a drone) (Li et al., 2022), aerospace structures, such as SpiderFab for large structures (Tian et al., 2022),

along with spare parts for aerospace components, such as engines (Shahrubudin et al., 2019).
- Robotic, mold, and prototype industries: Robotic arms (Li et al., 2022) and tools for vehicle maintenance (Li et al., 2022).
- Infrastructure and construction industry: Footbridges (Li et al., 2022).
- Automotive Industry: 3D-printed electric cars and buses called OLLI by Local Motor (Shahrubudin et al., 2019).
- Medical devices, tissue engineering, and wound dressing (Bi and Huang, 2022).
- Others: bicycle frames (Li et al., 2022).

Several applications are known for 3D-printed biomass-filled PLA composites:

- Providing a wood-like appearance for furniture and architecture models that has excellent scratch and wear resistance (Bhagia et al., 2021), such as the bamboo-PLA installation at Design Miami 2016 printed at the Manufacturing Demonstration Facility at Oak Ridge National Laboratory, or 3D printed biomass waste-PLA chairs with thermoplastic elastomer cushions.
- 3D printed cellulose materials used for medical applications: Tissue engineering and drug delivery (Wang et al., 2018).
- Electronics applications: Flexible electronics, such as batteries, supercapacitors, wearable electronics, and sensors (Wang et al., 2018).
- Smart packaging and textile applications (Wang et al., 2018).

However, concrete applications for continuous plant-reinforced bio-composites are still lacking. Nevertheless, there is huge potential in various other sectors: (1) the aerospace industry by using, for example, 4D-printed CNFRCs with controllable self-deformation in response to external conditions (Le Duigou et al., 2020); (2) automotive (door trims); (3) biomedical, such as medical instruments and models for visualization, education, and communication; (4) architecture, (5) building and construction industries; and (6) fashion industry, by using intelligent textile biofabrics.

4.8 Conclusions

CNFRCs possess attractive properties, such as being lightweight, environmental friendly, recyclable, and having achievable mechanical performance derived from plant fibers. The utilization of 3D printing, especially the FFF process, for CNFRCs with the capability of complex structural design and advanced actuation performance, has the potential to transform and significantly expand their applications in the future. The market for CNFRCs is quite promising, particularly in sectors such as automotive, civil engineering, sports, and biomedical fields.

However, despite its bright future, several challenges need to be addressed:

- Improving the current techniques of fiber impregnation cited previously in the technology landscape, including (1) the development of a cut fiber system to enable the creation of complex structural lightweight designs, and (2) controlling printing pressure through innovations such as a compaction roller or local laser heating of interfacial layer.

- Enhancing interfacial bonding by implementing surface fiber treatments or modifying the quality of yarn fibers and rheology of the polymer matrix to reduce void content and other defects that affect mechanical properties.

After extensive research and analysis of crucial parameters listed in the present chapter, the fishbone diagram (Fig. 4.6) was illustrated to demonstrate the build orientation, infill geometry, feed rate, and stacking sequence that need to be more deeply explored for the mechanical properties of FFF-printed CNFRCs.

Future research trends should focus on two main areas: materials and structures. In terms of materials, flax and pineapple leaf fibers show promising potential for the FFF process. This is also true for the PLA matrix that is commonly used because of its easy printability and interesting mechanical properties. Moreover, fully recyclable FFF-printed green composites and multimaterial composites customized with novel functionalities are envisioned as the future of novel CNFRCs. In terms of structures, lightweight bio-composite and bio-inspired complex structures for well-defined applications should be explored for their mechanical and dynamic properties, using machine learning and artificial intelligence to facilitate, optimize, and fasten the FFF process.

In conclusion, the application potential of CNFRCs in 3D printing remains largely untapped, which could elevate the FFF process to new heights through the combined advancement in both technology and materials. It is anticipated that the present chapter will inspire researchers and scholars to further investigate CNFRCs for their potential applications in the engineering industry.

References

Additive manufacturing (2015). *General Principles—Overview of process categories and feedstock*. ISO/ASTM International Standard. 17296−2:2015(E).

Agaliotis, E. M., Ake-Concha, B. D., May-Pat, A., Morales-Arias, J. P., Bernal, C., Valadez-Gonzalez, A., Herrera-Franco, P. J., Proust, G., Koh-Dzul, J. F., & Carrillo, J. G. (2022). Tensile behavior of 3D printed polylactic acid (PLA) based composites reinforced with natural fiber. *Polymers*, *14*, 3976. Available from https://doi.org/10.3390/polym14193976.

Ahmad, M. N., Ishak, M. R., Taha, M. M., Mustapha, F., Leman, Z., Lukista, D. D. A., Irianto., & Ghazali, I. (2022). Application of taguchi method to optimize the parameter of fused deposition modeling (FDM) using oil palm fiber reinforced thermoplastic composites. *Polymers*, *14*, 2140. Available from https://doi.org/10.3390/polym14112140.

Ahmed, W., Alnajjar, F., Zaneldin, E., Al-Marzouqi, A. H., Gochoo, M., & Khalid, S. (2020). Implementing FDM 3D printing strategies using natural fibers to produce biomass composite. *Materials*, *13*, 4065. Available from https://doi.org/10.3390/ma13184065.

Aida, H. J., Nadlene, R., Mastura, M. T., Yusriah, L., Sivakumar, D., & Ilyas, R. A. (2021). Natural fiber filament for Fused Deposition Modelling (FDM): A review. *International Journal of Sustainable Engineering*, *14*(6), 1988−2008. Available from https://doi.org/10.1080/19397038.2021.1962426.

Akil, H. M., Omar, M. F., Mazuki, A. A. M., Safiee, S., Ishak, Z. A. M., & Bakar, A. Abu (2011). Kenaf fiber reinforced composites: A review. *Materials and Design*, *32*(8−9), 4107−4121. Available from https://doi.org/10.1016/j.matdes.2011.04.008.

Akter, M., Uddin, M. H., & Anik, H. R. (2023). Plant fiber-reinforced polymer composites: A reviewon modification, fabrication, properties, and applications. *Polymer Bulletin*. Available from https://doi.org/10.1007/s00289-023-04733-5.

Auffray, L., Gouge, P.-A., & Hattali, L. (2022). Design of experiment analysis on tensile properties of PLA samples produced by fused filament fabrication. *The International Journal of Advanced Manufacturing Technology*, *118*, 4123−4137. Available from https://doi.org/10.1007/s00170-021-08216-7.

Badouard, C., Traon, F., Denoual, C., Mayer-Laigle, C., Païs, G., & Bourmaud, A. (2019). Exploring mechanical properties of fully compostable flax reinforced composite filaments for 3D printing applications. *Industrial Crops and Products.*, *135*, 246−250.

Baghaei, B., Skrifvars, M., Salehi, M., Bashir, T., Rissanen, M., & Nousiainen, P. (2014). Novel aligned hemp fiber reinforcement for structural biocomposites: Porosity, water absorption, mechanical performances and viscoelastic behaviour. *Composites: Part A*, *61*, 1−12.

Bakhtiari, H., Aamir, M., & Tolouei-Rad, M. (2023). Effect of 3D printing parameters on the fatigue properties of parts manufactured by fused filament fabrication: A review. *Applied Sciences*, *13*, 904. Available from https://doi.org/10.3390/app13020904.

Balla, V. K., Kate, K. H., Satyavolu, J., Singh, P., & Tadimeti, J. G. D. (2019). Additive manufacturing of natural fiber reinforced polymer composites: Processing and prospects. *Composites Part B: Engineering*, *174*, 106956. Available from https://doi.org/10.1016/j.compositesb.2019.106956.

Bhagia, S., Bornani, K., Agrawal, R., Satlewal, A., Durkovic, J., Lagana, R., Bhagia, M., Yoo, C. G., Zhao, X., Kunc, V., Pu, Y., Ozcan, S., & Ragauskas, A. J. (2021). Critical review of FDM 3D printing of PLA biocomposites filled with biomass resources, characterization, biodegradability, upcycling and opportunities for biorefineries. *Applied Materials Today*, *24*, 101078. Available from https://doi.org/10.1016/j.apmt.2021.101078.

Bi, X., & Huang, R. (2022). 3D printing of natural fiber and composites: A state-of-the-art review. *Materials & Design*, *222*, 111065. Available from https://doi.org/10.1016/j.matdes.2022.111065.

Bourmaud, A., Le Duigou, A., Gourier, C., & Baley, C. (2016). Influence of processing temperature on mechanical performance of unidirectional polyamide 11−flax fiber composites. *Industrial Crops and Products*, *84*, 151−165. Available from https://doi.org/10.1016/j.indcrop.2016.02.007.

Cai, R., Lin, H., Cheng, P., Zhang, Z., Wang, K., Peng, Y., Wu, Y., & Ahzi, S. (2022). Investigation on dynamic strength of printed continuous ramie fiber reinforced biocomposites at various strain rates using machine learning methods. *Polymer Composites*, *43*, 5235−5249. Available from https://doi.org/10.1002/pc.26816.

Cai, R., Wen, W., Wang, K., Peng, Y., Ahzi, S., & Chinesta, F. (2022). Tailoring interfacial properties of 3D-printed continuous natural fiber reinforced polypropylene composites through parameter optimization using machine learning methods. *Materials Today Communications*, *32,* 103985. Available from https://doi.org/10.1016/j.mtcomm.2022.103985.

Cheng, P., Wang, K., Chen, X., Wang, J., Peng, Y., Ahzi, S., & Chen, C. (2021). Interfacial and mechanical properties of continuous ramie fiber reinforced biocomposites fabricated by in-situ impregnated 3D printing. *Industrial Crops & Products*, *170,* 113760. Available from https://doi.org/10.1016/j.indcrop.2021.113760.

Christiyan, K. J., Chandrasekhar, U., & Venkateswarlu, K. (2016). A study on the influence of process parameters on the mechanical properties of 3D printed ABS composite. *IOP Conference Series: Materials Science and Engineering*, *114*, 012109.

Coroller, G., Lefeuvre, A., Le Duigou, A., Bourmaud, A., Ausias, G., Gaudry, T., & Baley, C. (2013). Effect of flax fibers individualisation on tensile failure of flax/epoxy unidirectional composite. *Composites Part A: Applied Science and Manufacturing*, *51*, 62−70. Available from https://doi.org/10.1016/j.compositesa.2013.03.018.

Couture, A., Lebrun, G., & Laperrière, L. (2016). Mechanical properties of polylactic acid (PLA) composites reinforced with unidirectional flax and flax-paper layers. *Composite Structures*, *154*, 286−295. Available from https://doi.org/10.1016/j.compstruct.2016.07.069.

Depuydt, D., Balthazar, M., Hendrickx, K., Six, W., Ferraris, E., Desplentere, F., Ivens, J., & Van Vuure, A. W. (2019). Production and characterization of bamboo and flax fiber reinforced polylactic acid filaments for fused deposition modeling (FDM). *Polymer Composites*, *40*, 1951−1963.

Dey, A., Roan Eagle, I. N., & Yodo, N. (2021). A review on filament materials for fused filament fabrication. *Journal of Manufacturing and Materials Processing*, *5*, 69. Available from https://doi.org/10.3390/jmmp5030069.

Eichenhofer, M., Wong, J. C. H., & Ermanni, P. (2017). Continuous lattice fabrication of ultra-lightweight composite structures. *Additive Manufacturing*, *18*, 48−57. Available from https://doi.org/10.1016/j.addma.2017.08.013.

Fruleux, T., Castro, M., Correa, D., Wang, K., Matsuzaki, R., & Le Duigou, A. (2022). Geometric limitations of 3D printed continuous flax-fiber reinforced biocomposites cellular lattice structures. *Composites Part C*, *8*. Available from https://doi.org/10.1016/j.jcomc.2022.100313.

Gautreau, M., Kervoelen, A., Barteau, G., Delattre, F., Colinart, T., Pierre, F., Hauguel, M., Le Moigne, N., Guillon, F., Bourmaud, A., & Beaugrand, J. (2021). Fiber individualisation and mechanical properties of a Flax-PLA non-woven composite following physical pre-treatments. *Coatings*, *11*, 846. Available from https://doi.org/10.3390/coatings11070846.

Gibson, I., Rosen, D., & Stucker, B. (2015). *Additive manufacturing technologies: 3D printing, rapid prototyping, and direct digital manufacturing* (Second ed). Springer-Verlag Publ. New York. Available from https://doi.org/10.1007/978-1-4939-2113-3.

Guo, N., & Leu, M. C. (2013). Additive manufacturing: Technology, applications and research needs. *Frontiers of Mechanical Engineering*, *8*, 215−243.

Hao, W., Liu, Y., Zhou, H., Chen, H., Fang, D., 2018. Preparation and characterization of 3D printed continuous carbon fiber reinforced thermosetting composites, Polymer Testing 65, 29−34.

Hou, Z., Tian, X., Zhang, J., & Li, D. (2018). 3D printed continuous fiber reinforced composite corrugated structure. *Composite Structures*, *184*, 1005−1010. Available from https://doi.org/10.1016/j.compstruct.2017.10.080.

Hu, Q., Duan, Y., Zhang, H., Liu, D., Yan, B., & Peng, F. (2018). Manufacturing and 3D printing of continuous carbon fiber prepreg filament. *Journal of Materials Science*, *53*, 1887−1898. Available from https://doi.org/10.1007/s10853-017-1624-2.

ISO/ASTM52900–2021, Additive manufacturing, General principles, Fundamentals and vocabulary.

Jagadish., Rajakumaran, M., & Ray, A. (2020). Investigation on mechanical properties of pineapple leaf-based short fiber-reinforced polymer composite from selected Indian (northeastern part) cultivars. *Journal of Thermoplastic Composite Materials*, *33*(3), 324−342.

Kabir, S. M. F., Mathur, K., & Seyam, A.-F. M. (2020). A critical review on 3D printed continuous fiber-reinforced composites: History, mechanism, materials and properties. *Composite Structures*, *232*, 111476. Available from https://doi.org/10.1016/j.compstruct.2019.111476.

Karimah, A., Ridho, M. R., Munawar, S. S., Adi, D. S., Ismadi., Damayanti, R., Subiyanto, B., Fatriasari, W., & Fudholi, A. (2021). A review on natural fibers for development of eco-friendly bio-composite: Characteristics, and utilizations. *Journal of Materials Research and Technology*, *13*, 2442−2458. Available from https://doi.org/10.1016/j.jmrt.2021.06.014.

Kariz, M., Sernek, M., Obućina, M., & Kuzman, M. K. (2018). Effect of wood content in FDM filament on properties of 3D printed parts. *Materials Today Communications*, *14*, 135−140.

Krajangsawasdi, N., Blok, L. G., Hamerton, I., Longana, M. L., Woods, B. K. S., & Ivanov, D. S. (2021). Fused deposition modelling of fiber reinforced polymer composites: A parametric review. *Journal of Composites Science.*, *5*, 29. Available from https://doi.org/10.3390/jcs5010029.

Krishna, K. V., & Kanny, K. (2016). The effect of treatment on kenaf fiber using green approach and their reinforced epoxy composites. *Composites Part B: Engineering*, *104*, 111−117. Available from https://doi.org/10.1016/j.compositesb.2016.08.010.

Kuschmitz, S., Schirp, A., Busse, J., Watschke, H., Schirp, C., & Vietor, T. (2021). Development and processing of continuous flax and carbon fiber-reinforced thermoplastic composites by a modified material extrusion process. *Materials*, *14*, 2332. Available from https://doi.org/10.3390/ma14092332.

Lanzotti, A., Pei, E., Grasso, M., Staiano, G., & Martorelli, M. (2015). The impact of process parameters on mechanical properties of parts fabricated in PLA with an open-source 3-D printer. *Rapid Prototyping Journal*, *21*, 604−617.

Le Duigou, A., Barbé, A., Guillou, E., & Castro, M. (2019). 3D printing of continuous flax fiber reinforced biocomposites for structural applications. *Materials and Design*, *180*107884. Available from https://doi.org/10.1016/j.matdes.2019.107884.

Le Duigou, A., Chabaud, G., Matsuzaki, R., & Castro, M. (2020). Tailoring the mechanical properties of 3D-printed continuous flax/PLA biocomposites by controlling the slicing parameters. *Composites Part B: Engineering*, *203*, 108474. Available from https://doi.org/10.1016/j.compositesb.2020.108474.

Le Duigou, Antoine, Correa, D., Ueda, M., Matsuzaki, R., & Castro, M. (2020). A review of 3D and 4D printing of natural fiber biocomposites. *Materials & Design*, *194*, 108911. Available from https://doi.org/10.1016/j.matdes.2020.108911.

Le Guen, M., Hill, S., Smith, D., Theobald, B., Gaugler, E., Barakat, A., & Mayer-Laigle, C. (2019). Influence of rice husk and wood biomass properties on the manufacture of filaments for fused deposition modeling. *Frontiers in Chemistry.*, *7*, 735.

Lee, C. H., Padzil, F. N. B. M., Lee, S. H., Ainun, Z. M. A., & Abdullah, L. C. (2021). Potential for natural fiber reinforcement in pla polymer filaments for fused deposition modeling (Fdm) additive manufacturing: A review. *Polymers*, *13*, 1407.

Li, J., Durandet, Y., Huang, X., Sun, G., & Ruan, D. (2022). Additively manufactured fiber-reinforced composites: A review of mechanical behavior and opportunities. *Journal of Materials Science & Technology*, *119*, 219−244. Available from https://doi.org/10.1016/j.jmst.2021.11.063.

Li, M., Pu, Y., Thomas, V. M., Yoo, Ch. G., Ozcan, S., Deng, Y., Nelson, K., & Ragauskas, A. J. (2020). Recent advancements of plant-based natural fiber−reinforced composites and their applications. *Composite Part B*, *200,* 108254. Available from https://doi.org/10.1016/j.compositesb.2020.108254.

Liu, S., Li, Y., & Li, N. (2018). A novel free-hanging 3D printing method for continuous carbon fiber reinforced thermoplastic lattice truss core structures. *Materials & Design*, *137*, 235−244. Available from https://doi.org/10.1016/j.matdes.2017.10.007.

Long, Y., Zhang, Z., Fu, K., & Li, Y. (2021). Efficient plant fiber yarn pre-treatment for 3D printed continuous flax fiber/poly(lactic) acid composites. *Composites Part B: Engineering*, *227*, 109389. Available from https://doi.org/10.1016/j.compositesb.2021.109389.

Lu, L., Hou, J., Yuan, S., Yao, X., Li, Y., & Zhu, J. (2023). Deep learning-assisted real-time defect detection and closed-loop adjustment for additive manufacturing of continuous fiber-reinforced polymer composites. *Robotics and Computer-Integrated Manufacturing*, *79*, 102431. Available from https://doi.org/10.1016/j.rcim.2022.102431.

MarkForged. MarkForged Visual Troubleshooting Guide. Available online: https://support.markforged.com/hc/en-us/articles/205927119-MarkForged-Visual-Troubleshooting-Guide (accessed on 30.03.23).

Marrot, L., Bourmaud, A., Bono, P., & Baley, C. (2014). Multi-scale study of the adhesion between flax fibers and biobased thermoset matrices. *Materials and Design*. Available from http://doi.org/10.1016/j.matdes.2014.04.087.

Mashayekhi, F., Bardon, J., Berthé, V., Perrin, H., Westermann, S., & Addiego, F. (2021). Fused filament fabrication of polymers and continuous fiber-reinforced polymer composites: Advances in structure optimization and health monitoring. *Polymers*, *13*, 789. Available from https://doi.org/10.3390/polym13050789.

Matsuzaki, R., Ueda, M., Namiki, M., Jeong, T.-K., Asahara, H., Horiguchi, K., Nakamura, T., Todoroki, A., & Hirano, Y. (2016). Three-dimensional printing of continuous-fiber composites by in-nozzle impregnation. *Scientific Reports*, *6*, 23058. Available from https://doi.org/10.1038/srep23058.

Monti, A. (2016). Elaboration et caractérisation mécanique d'une structure composite sandwiché à base de constituants naturels. Acoustique [physics.class-ph]. Université du Maine. Français. NNT: 2016LEMA1023.

Oksman, K. (2001). High quality flax fiber composites manufactured by the resin transfer moulding process. *Journal of Reinforced Plastics and Composites*, *20*, 621. Available from https://doi.org/10.1177/073168401772678634.

Pantaloni, D., Rudolph, A. L., Shah, D. U., Baley, C., & Bourmaud, A. (2021). Interfacial and mechanical characterisation of biodegradable polymer-flax fiber composites. *Composites Science and Technology*, *201,* 108529. Available from https://doi.org/10.1016/j.compscitech.2020.108529.

Pickering, K. L., Aruan Efendy, M. G., & Le, T. M. (2015). A review of recent developments in natural fiber composites and their mechanical performance. *Review, Composite Part A*, *83*, 98−112. Available from https://doi.org/10.1016/j.compositesa.2015.08.038.

Pruß, H., & Vietor, T. (2015). Design for fiber-reinforced additive manufacturing. *Journal of Mechanical Design*, *137*, 111409. Available from https://doi.org/10.1115/1.4030993.

Quan, C., Han, B., Hou, Z., Zhang, Q., Tian, X., & Lu, T. J. (2020). 3d printed continuous fiber reinforced composite auxetic honeycomb structures. *Composites Part B: Engineering*, *187*, 107858. Available from https://doi.org/10.1016/j.compositesb.2020.107858.

Rajendran Royan, N. R., Leong, J. S., Chan, W. N., Tan, J. R., & Shamsuddin, Z. S. B. (2021). Current state and challenges of natural fiber-reinforced polymer composites as feeder in Fdm-based 3d printing. *Polymers*, *13*, 2289.

Ravi, A. K., Deshpande, A., & Hsu, K. H. (2016). An in-process laser localized pre-deposition heating approach to inter-layer bond strengthening in extrusion based polymer additive manufacturing. *Journal of Manufacturing Processes*, *24*, 179−185. Available from https://doi.org/10.1016/j.jmapro.2016.08.007.

Rivero-Romero, O., Barrera-Fajardo, I., & Unfried-Silgado, J. (2023). Effects of printing parameters on fiber eccentricity and porosity level in a thermoplastic matrix composite reinforced with continuous banana fiber fabricated by FFF with in situ impregnation. *The International Journal of Advanced Manufacturing Technology*, *125*, 1893−1901. Available from https://doi.org/10.1007/s00170-022-10799-8.

Saba, N., Paridah, M. T., & Jawaid, M. (2015). Mechanical properties of kenaf fiber reinforced polymer composite: A review. *Construction and Building Materials*, *76*, 87−96. Available from https://doi.org/10.1016/j.conbuildmat.2014.11.043.

Shah, D. U. (2013). Developing plant fiber composites for structural applications by optimising composite parameters: A critical review. *Review, Journal of Materials Science*, *48*, 6083−6107. Available from https://doi.org/10.1007/s10853-013-7458-7.

Shahrubudin, N., Lee, T. C., & Ramlan, R. (2019). An overview on 3D printing technology: Technological, materials, and applications. *Procedia Manufacturing*, *35*, 1286−1296. Available from https://doi.org/10.1016/j.promfg.2019.06.089.

Singh, R., Kumar, R., & Ranjan, N. (2017). Sustainability of recycled ABS and PA6 by banana fiber reinforcement: Thermal, mechanical and morphological properties. *Journal of The Institution of Engineers (India): Series C*. Available from https://doi.org/10.1007/s40032-017-0435-1.

Stoof, D., & Pickering, K. (2018). Sustainable composite fused deposition modelling filament using recycled pre-consumer polypropylene. *Composites Part B: Engineering*, *135*, 110−118.

Sugiyama, K., Matsuzaki, R., Ueda, M., Todoroki, A., & Hirano, Y. (2018). 3D printing of composite sandwich structures using continuous carbon fiber and fiber tension. *Composites Part A: Applied Science and Manufacturing*, *113*, 114−121. Available from https://doi.org/10.1016/j.compositesa.2018.07.029.

Suteja, J., Firmanto, H., Soesanti, A., & Christian, C. (2020). Properties investigation of 3D printed continuous pineapple leaf fiber-reinforced PLA composite. *Journal of Thermoplastic Composite Materials*, *35*, 1−10. Available from https://doi.org/10.1177/0892705720945371.

Tekinalp, H. L., Kunc, V., Velez-Garcia, G. M., Duty, C. E., Love, L. J., Naskar, A. K., Blue, C. A., & Ozcan, S. (2014). Highly oriented carbon fiber—Polymer composites via additive manufacturing. *Composites Science and Technology.*, *105*, 144−150.

Terekhina, S., Egorov, S., Tarasova, T., Skornyakov, I., Guillaumat, L., & Hattali, M. L. (2022). In-nozzle impregnation of continuous textile flax fiber/polyamide 6 composite during FFF process. *Composites Part A: Applied Science and Manufacturing*, *153*, 106725. Available from https://doi.org/10.1016/j.compositesa.2021.106725.

Terekhina, S., Tarasova, T., Egorov, S., Guillaumat, L., & Hattali, M. L. (2020a). On the difference in material structure and fatigue properties of polyamide specimens produced by fused filament fabrication and selective laser sintering. *The International Journal of Advanced Manufacturing Technology*, *111*, 93−107. Available from https://doi.org/10.1007/s00170-020-06026-x.

Terekhina, S., Tarasova, T., Egorov, S., Skornyakov, I., Guillaumat, L., & Hattali, L. (2021). Flexural quasi-static and fatigue behaviours of fused filament deposited PA6 and PA12 polymers. *The International Journal of Advanced Manufacturing Technology*, *117*, 2041−2048. Available from https://doi.org/10.1007/s00170-021-07223-y.

Terekhina, S., Tarasova, T., Egorov, S., Skornyakov, I., Guillaumat, L., & Hattali, M. L. (2020b). The effect of build orientation on both flexural quasi-static and fatigue behaviours of filament deposited PA6 polymer. *International Journal of Fatigue*, *140*, 105825. Available from https://doi.org/10.1016/j.ijfatigue.2020.105825.

Tian, X., Liu, T., Yang, C., Wang, Q., & Li, D. (2016). Interface and performance of 3D printed continuous carbon fiber reinforced PLA composites. *Composites Part A: Applied Science and Manufacturing.*, *88*, 198−205.

Tian, X., Todoroki, A., Liu, T., Wu, L., Hou, Z., Ueda, M., Hirano, Y., Matsuzaki, R., Mizukami, K., Iizuka, K., Malakhov, A. V., Polilov, A. N., Li, D., & Lu, B. (2022). 3D printing of continuous fiber reinforced polymer composites: Development, application, and prospective. *Chinese Journal of Mechanical Engineering: Additive Manufacturing Frontiers*, *1,* 100016. Available from https://doi.org/10.1016/j.cjmeam.2022.100016.

Tran, T. Q., Ng, F. L., Kai, J. T. Y., Feih, S., & Nai, M. L. S. (2022). Tensile strength enhancement of fused filament fabrication printed parts: A review of process improvement approaches and respective impact. *Additive Manufacturing*, *54,* 102724. Available from https://doi.org/10.1016/j.addma.2022.102724.

Ueda, M., Kishimoto, S., Yamawaki, M., Matsuzaki, R., Todoroki, A., Hirano, Y., & Le Duigou, A. (2020). 3D compaction printing of a continuous carbon fiber reinforced thermoplastic. *Composites Part A: Applied Science and Manufacturing*, *137*, 105985. Available from https://doi.org/10.1016/j.compositesa.2020.105985.

Vaneker, T. H. J. (2017). Material extrusion of continuous fiber reinforced plastics using commingled yarn. *Procedia CIRP*, *66*, 317−322. Available from https://doi.org/10.1016/j.procir.2017.03.367.

Wang, Q., Sun, J., Yao, Q., Ji, C., Liu, J., & Zhu, Q. (2018). 3D printing with cellulose materials. *Cellulose*, *25*, 4275−4301. Available from https://doi.org/10.1007/s10570-018-1888-y.

Wang, Y., Weng, Y., & Wang, L. (2014). Characterization of interfacial compatibility of polylactic acid and bamboo flour (PLA/BF) in biocomposites. *Polymer Testing*, *36*, 119−125.

Wegst, U. G. K., Bai, H., Saiz, E., Tomsia, A. P., & Ritchie, R. O. (2015). Bioinspired structural materials. *Nature Materials*, *14*, 23−36. Available from https://doi.org/10.1038/nmat4089.

Wickramasinghe, S., Do, T., & Tran, P. (2020). FDM-based 3D printing of polymer and associated composite: A review on mechanical properties, defects and treatments. *Polymers*, *12*, 1529. Available from https://doi.org/10.3390/polym12071529.

Williams, D. (1990). An introduction to medical and dental materials. In. In D. Williams (Ed.), *Concise encyclopedia of medical and dental materials* (pp. 17−20). Oxford, UK: Pergamon Press.

Yan, L., Chouw, N., & Jayaraman, K. (2014). Flax fiber and its composites-A review. *Composites Part B: Engineering*, *56*, 296−317. Available from https://doi.org/10.1016/j.compositesb.2013.08.014.

Yao, Y., Li, M., Lackner, M., & Herfried, L. (2020). A continuous fiber-reinforced additive manufacturing processing based on PET fiber and PLA. *Materials*, *13*, 3044. Available from https://doi.org/10.3390/ma13143044.

Yu, T., Hu, C., Chen, X., & Li, Y. (2015). Effect of diisocyanates as compatibilizer on the properties of ramie/poly(lactic acid) (PLA) composites. *Composites Part A: Applied Science and Manufacturing*, *76*, 20−27. Available from https://doi.org/10.1016/j.compositesa.2015.05.010.

Zhang, H., Liu, D., Huang, T., Hu, Q., & Lammer, H. (2020). Three-dimensional printing of continuous flax fiber-reinforced thermoplastic composites by five-axis machine. *Materials*, *13*, 1678. Available from https://doi.org/10.3390/ma13071678.

Zhang, L., Lv, S., Sun, C., Wan, L., Tan, H., & Zhang, Y. (2017). Effect of MAH-g-PLA on the properties of wood fiber/polylactic acid composites. *Polymers*, *9*, 591. Available from https://doi.org/10.3390/polym9110591.

Zhang, M., Tian, X., Cao, H., Liu, T., Akmal Zia, A., & Li, D. (2023). 3D printing of fully recyclable continuous fiber self-reinforced composites utilizing supercooled polymer melts. *Composites Part A: Applied Science and Manufacturing*, *169*, 107513. Available from https://doi.org/10.1016/j.compositesa.2023.107513.

Zhang, W., Cotton, C., Sun, J., Heider, D., Gu, B., Sun, B., & Chou, T.-W. (2018). Interfacial bonding strength of short carbon fiber/acrylonitrile-butadiene-styrene composites fabricated by fused deposition modeling. *Composites Part B: Engineering*, *137*, 51–59.